Inhibitory Antibodies to Human Angiotensin-Converting Enzyme: Fine Epitope Mapping and Mechanism of Action†

Olga E. Skirgello,[‡,§] Irina V. Balyasnikova,[§,||] Petr V. Binevski,[‡] Zhu-Li Sun,[||] Igor I. Baskin,[‡] Vladimir A. Palyulin,[‡] Andrei B. Nesterovitch,[⊥] Ronald F. Albrecht, II,[||] Olga A. Kost,[‡,#] and Sergei M. Danilov*[,||,#]

Department of Chemistry, Moscow State University, Russia, Department of Anesthesiology, University of Illinois at Chicago, Chicago, Illinois 60612, and Department of Orthopedic Surgery, Rush University Medical Center, Chicago, Illinois 60612

Received December 20, 2005; Revised Manuscript Received February 16, 2006

ABSTRACT: Angiotensin I-converting enzyme (ACE), a key enzyme in cardiovascular pathophysiology, consists of two homologous domains (N and C), each bearing a Zn-dependent active site. We modeled the 3D-structure of the ACE N-domain using known structures of the C-domain of human ACE and the ACE homologue, ACE2, as templates. Two monoclonal antibodies (mAb), 3A5 and i2H5, developed against the human N-domain of ACE, demonstrated anticatalytic activity. N-domain modeling and mutagenesis of 21 amino acid residues allowed us to define the epitopes for these mAbs. Their epitopes partially overlap: amino acid residues K407, E403, Y521, E522, G523, P524, D529 are present in both epitopes. Mutation of 4 amino acid residues within the 3A5 epitope, N203E, R550A, D558L, and K557Q, increased the apparent binding of mAb 3A5 with the mutated N-domain 3-fold in plate precipitation assay, but abolished the inhibitory potency of this mAb. Moreover, mutation D558L dramatically decreased 3A5-induced ACE shedding from the surface of CHO cells expressing human somatic ACE. The inhibition of N-domain activity by mAbs 3A5 and i2H5 obeys similar kinetics. Both mAbs can bind to the free enzyme and enzyme−substrate complex, forming E·mAb and E·S·mAb complexes, respectively; however, only complex E·S can form a product. Kinetic analysis indicates that both mAbs bind better with the ACE N-domain in the presence of a substrate, which, in turn, implies that binding of a substrate causes conformational adjustments in the N-domain structure. Independent experiments with ELISA demonstrated better binding of mAbs 3A5 and i2H5 in the presence of the inhibitor lisinopril as well. This effect can be attributed to better binding of both mAbs with the "closed" conformation of ACE, therefore, disturbing the hinge-bending movement of the enzyme, which is necessary for catalysis.

Angiotensin I-converting enzyme (ACE[1]) (EC 3.4.15.1, CD 143) is a zinc-metallopeptidase, responsible for the formation of the vasoconstrictor angiotensin II and the inactivation of the vasodilator bradykinin. The enzyme is also involved in neuropeptide metabolism and reproductive and immune functions (for reviews see refs *1*−*4*). The somatic isoform is expressed widely at surface−fluid interfaces and plays an important role in blood pressure regulation, the development of vascular pathology, and endothelium remodeling in some disease states. ACE has been assigned as a CD marker: CD 143 (*5*, *6*). The testicular isoform is limited to spermatozoa and is essential for male fertility (*7*).

Somatic ACE consists of two homologous N- and C-domains, each having a functional active site (*8*). The tertiary structure of somatic ACE is still unknown. Testicular ACE is coded by the same gene as somatic ACE but from an alternative promoter (*9*). This ACE is identical to the C-terminal domain of somatic enzyme, except for a short N-terminal sequence of 36 amino acids, and thus contains only one catalytic site (*10*). The crystal structure of the human C-terminal domain was recently described (*11*). Somatic and testicular ACEs are both type 1 integral membrane-anchored proteins. Somatic ACE also exists as a soluble form, e.g., in plasma, cerebrospinal fluid, and seminal plasma (see reviews *1*−*3*), that lacks the transmembrane domain responsible for membrane attachment (*12*−*16*).

The "bridge sequence" between the two ACE domains can be cleaved both in vivo and in vitro (*17*−*21*). Different heat stabilities of the domains allow selective inactivation of the C-domain and underlie the method of acquiring an active N-domain with inactive C-domain within a full-length ACE (*19*, *21*). These results suggest that the two domains within the somatic ACE molecule are rather separate and distinctive structures.

† This work was supported in part by Russian Foundation for Basic Research, Grant 03-04-48821 (to O.A.K.).

* Corresponding author. Mailing address: Anesthesiology Research Center, University of Illinois at Chicago, 1819 W. Polk St. (M/C 519), Chicago, IL 60612. Phone: (312) 413-7526. Fax: (312) 996-9680. E-mail: danilov@uic.edu.

‡ Moscow State University.

§ Equally contributed to this work.

|| University of Illinois at Chicago.

⊥ Rush University Medical Center.

Authors share equal seniority over this paper.

[1] Abbreviations: ACE, angiotensin converting enzyme; Hip-His-Leu, hippuryl-L-histidyl-L-leucine; Z-Phe-His-Leu, benzyloxycarbonyl-phenylalanyl-L-histidyl-L-leucine; CHO, Chinese hamster ovary; mAb, monoclonal antibody; ELISA, enzyme-linked immunosorbent assay; CD markers, cluster designation markers; PBS, phosphate-buffered saline; (CHAPS), 3-[(3-cholamidopropyl)-dimethylammonio]-1-propanosulfonate; TMB, tetramethylbenzidine.

10.1021/bi052591h CCC: $33.50
Published on Web 03/22/2006

Hydrolysis of various substrates by different ACE forms and, especially, the inhibition of ACE by inhibitors have been studied intensively (*3*, *20*, *22*−*27*). Special attention was paid to the differences in the function of N- and C-domains of ACE, as well as to the development of ACE inhibitors specific for each domain (*20*, *28*−*33*). The two catalytic centers within somatic ACE were long considered to function independently (*22*, *24*, *28*, *34*). However, our recent studies with both bovine and human ACE (*20*, *27*) revealed the existence of strong negative cooperativity between the N- and C-domain active centers functioning in full-length ACE, which implies tight proximity of the domains within the somatic enzyme molecule.

Development of numerous mAbs to different epitopes of the ACE molecule which influence ACE functions, in conjunction with epitope mapping, provides a unique opportunity to study ACE in fine structural detail. Thus, the study of the effect of mAbs on ACE shedding (*35*) or ACE dimerization in reverse micelles (*36*) plus epitope mapping of functionally active antibodies allowed us to identify the region on the N-domain that determines a low rate of somatic ACE shedding from the cell surface (*36*). One of the mAbs, 3A5, which greatly influences ACE shedding (*35*), also demonstrated strong anticatalytic activity (*25*).

The presence of anti-ACE autoantibodies was indicated recently in several diseases with an autoimmune component: lupus erythrematosis, scleroderma, and rheumatoid arthritis (*35*, *38*). The clinical significance of the presence of these autoantibodies is still unclear. However, we might assume that an epitope specificity of the autoantibodies to ACE for these distinct diseases could be a characteristic of the pathology.

In this study we identified the epitopes for two mAbs that exhibit inhibitory activity toward the N-domain of ACE. Detailed kinetic analysis of ACE inhibition by these mAbs allowed us to reveal their mechanisms of action. Modeling of the N-domain structure along with the knowledge of these kinetic mechanisms of inhibition allowed us to hypothesize about a mechanism action of the enzyme.

MATERIALS AND METHODS

Chemicals. Benzyloxycarbonyl-L-phenylalanyl-L-histidyl-L-leucine (Z-Phe-His-Leu) was from Bachem (King of Prussia, PA). Hippuryl-L-histidyl-L-leucine (Hip-His-Leu), *N*-(*S*-1-carboxy-3-phenylpropyl)-L-lysyl-L-proline (lisinopril) and other reagents (unless otherwise indicated) were obtained from Sigma (St. Louis, MO).

Expression of Human ACE Constructs in CHO Cells. Stable cell lines of CHO cells expressing wild-type human somatic ACE (clone 2C2) or single N-domain of ACE (D629-clone 4G6) were cultured as described previously (*39*, *40*). CHO-ACE cells at confluence were washed gently with PBS and incubated 24−48 h with "complete culture medium" (Mediatech, Inc., Herndon, VA) without FBS. Culture medium was collected as a source of soluble ACE, whereas a cell lysate prepared with 8 mM CHAPS was a source of the membrane-bound form of ACE (*35*, *39*).

Purified N-domain of human ACE was obtained by limited proteolysis of the parent pure somatic ACE after partial denaturation in NH_4OH solution as described in ref *41*. N-Domain preparations proved to be homogeneous according to SDS−PAGE electrophoresis. Stoichiometric titration of active molecules in solutions of N-domain of ACE was performed with the specific competitive inhibitor lisinopril as described in refs *27*, *41*.

Antibodies. Properties of a set of monoclonal antibodies directed to different epitopes located on the N-domain of ACE were described in detail elsewhere (*25*, *35*−*37*, *39*, *40*).

ACE activity was assayed fluorimetrically with different substrates, Hip-His-Leu and Z-Phe-His-Leu, as described (*42*, *43*).

Inhibitory action of anti-ACE mAbs was tested using single N-domain as well as numerous mutants of recombinant truncated N-domain and somatic ACE, membrane-bound and soluble. ACEs with enzymatic activity of around 10 mU/mL (with Hip-His-Leu or Z-Phe-His-Leu) were incubated with different concentrations of mAbs in 10 mM phosphate buffer saline, pH 7.4, containing 150 mM NaCl with 0.1 mg/mL bovine serum albumin, for 2 h at 25 °C, then 20−40 μL of the reaction mixture was added to 200 μL of substrate (5 mM Hip-His-Leu or 2 mM Z-Phe-His-Leu) in the potassium phosphate buffer (100 mM), pH 8.3, containing 300 mM NaCl and 80 mM $ZnS0_4$ (PBS-I), and the residual ACE activity was determined.

In some experiments the reaction mixtures (475 μL) containing 0.1 nM N-domain and 0−7 nM mAbs in 50 mM phosphate buffer, pH 7.5, containing 150 mM KCl and 1 μM $ZnCl_2$ (PBS-II), were incubated for 2 h at 25 °C. Residual enzyme activities were then determined by adding 25 μL of 3.2 mM Hip-His-Leu or 2 mM Z-Phe-His-Leu and measuring the initial rates of hydrolysis. The influence of pH on the inhibitory action of mAbs on the N-domain of ACE was determined at two mAb concentrations, 0.7 nM and 3.0 nM, in 15 mM acetate−15 mM phosphate−15 mM borate buffer, containing 0.15 M KCl and 1 μM $ZnCl_2$.

Kinetic studies of the inhibitory action of mAbs 3A5 and i2H5 were performed with the N-domain of ACE obtained by limited proteolysis of somatic enzyme. The reaction mixture containing 0.1 nM N-domain and 0−10 nM mAbs in PBS-II was incubated for 2 h at 25 °C. This preincubation time was proved to be sufficient for establishing equilibrium between enzyme and mAb. The N-domain of ACE was found to be stable under these conditions. Residual ACE activity was then determined in duplicate with different concentrations (50−400 μM) of Hip-His-Leu. The mode of ACE inhibition by mAbs 3A5 and i2H5, as well as the values of the inhibition constants, was determined by data processing in Dixon coordinates, $1/v$ vs [mAb], and modified Cornish-Bowden coordinates, $[S]/v$ vs [mAb] (*44*, *45*).

Quantification of ACE Binding by Anti-ACE mAb (Plate Precipitation Assay and ELISA). Microtiter plates bound with goat-anti-mouse IgG were coated with different anti-ACE mAbs and were incubated with serum-free culture medium obtained from CHO-ACE cells (wild-type or mutants). In some experiments mAbs were adsorbed to the wells of microtiter plates directly, without the goat-anti-mouse bridge (*46*). In some experiments the incubation of ACEs with immobilized mAbs was performed in the presence of ACE inhibitor lisinopril or EDTA as well.

The amount of ACE precipitated by a given mAb (which reflects the affinity of binding) was quantified by two methods:

(i) Precipitated ACE activity was estimated in the wells using Hip-His-Leu or Z-Phe-His-Leu as substrate as described previously (*25*). The minor background hydrolysis of the substrate in the wells coated by non-immune mouse IgG was subtracted from each value obtained with specific anti-ACE mAbs.

(ii) The amount of precipitated ACE protein was quantified by incubation with sheep-anti-ACE polyclonal antibodies conjugated with horseradish peroxidase from ACE ELISA kit (Chemicon Int, Temecula, CA) followed by spectrophotometric assay with tetramethylbenzidine (TMB) as a substrate at 450 or 620 nm.

Quantification of Anti-ACE mAb Binding by the N-Domain of ACE (Direct ELISA). Microtiter plates coated with purified N-domain (10 μg/mL, 50 μL/well) were incubated with mAbs, 3A5 or i2H5. The amount of mAb (which reflects the affinity of binding) was quantified by incubation with rabbit-anti-mouse-IgG polyclonal antibodies conjugated with horseradish peroxidase (Imtek, Moscow, Russia) followed by spectrophotometric assay with TMB. In a separate set of experiments the incubation of mAbs with immobilized N-domain was performed in the presence of ACE inhibitor lisinopril.

Binding constants for mAb i2H5 and 3A5 were determined using purified N-domain adsorbed to plastic. In a separate experiment the binding constant for mAb 3A5 was determined using somatic ACE as well. The amount of adsorbed ACE was preliminarily estimated from its activity in microtiter wells and known kinetic parameters (*27*) for the hydrolysis of the substrate Z-Phe-His-Leu. The complete curves of ACE titration with mAbs were obtained. Concentrations of the ACE−mAb complex and of the free enzyme and free mAb were calculated from the direct ELISA data for each experimental point using the following relations:

$$P_m = \frac{P_b C_b + P_f C_f}{C_b + C_f} \quad (1)$$

$$C_f(E) = \mathrm{ACE}_0 - C_b \quad (2)$$

$$C_f = \mathrm{mAb}_0 - C_b \quad (3)$$

$$C_b = \frac{P_m - P_f}{P_b - P_f}\mathrm{ACE}_0 \quad (4)$$

where P_f is a peroxidase signal in the absence of mAb (which corresponds to the lower plateau value in the complete titration curve); P_b is a peroxidase signal at maximal concentration of the enzyme−inhibitor complex (the upper plateau value in the titration curve); P_m are the peroxidase signals determined at different concentrations of mAb; mAb_0 and ACE_0 are the total concentrations of mAb and of the N-domain, respectively; C_f and $C_f(E)$ are the equilibrium concentrations of the free mAb and enzyme; and C_b is the concentration of the ACE−mAb complex. The processing of C_b and C_f values in the C_b/C_f versus C_b coordinates, Scatchard's coordinates (*47*), provides the dissociation constant of the ACE−mAb complex.

Mutagenesis. For mutagenesis studies and following fine epitope mapping of mAbs 3A5 and i2H5, the truncated N terminal domain of human ACE containing the first 629 amino acid residues (D629) (and its cDNA) was used (*40*). A series of 21 single or double amino acid substitutions in cDNA for D629 was generated using a mutagenesis kit (Stratagene, La Jolla, CA). Mutants were identified and confirmed by DNA sequence analysis. Mutated variants of the truncated N-domain were expressed in CHO cells using lipofectamine as described (*39*). These constructs do not contain a transmembrane anchor; therefore the expressed ACE protein was secreted to the culture medium. Serum-free "complete culture medium" (see above) from these transfected cells was used as a source of the mutated variants of the N terminal domain of human ACE. These mutants are referred to by the single letter amino acid code for the wild-type protein (in our case D629), the position of this amino acid in the amino acid sequence, followed by the variant amino acid in single letter code, e.g., N203E is an asparagine (N) substitution by a glutamic acid (E) at position 203. In a separate experiment the D558L mutation was also generated in somatic, two domain ACE.

Cell ELISA. CHO-ACE cells were grown in 96-well plates until confluence, chilled on ice for at least 30 min, and washed several times with cold PBS. Control mouse IgG or anti-ACE mAbs (10 μg/mL in PBS-I-BSA) was added and incubated for 2 h on ice. After washing, cells were fixed with 4% paraformaldehyde for 15 min at room temperature and washed several times with PBS-I, before the bound mAbs (that reflect membrane-bound ACE) were quantified by incubation with alkaline phosphatase-conjugated anti-mouse IgG (Sigma, St. Louis, MO) followed by spectrophotometric assay with *p*-nitrophenylphosphate as a substrate at 405 nm.

ACE Shedding Assay. CHO-ACE cells were grown in 96-well microtiter plates. Once confluent, they were washed 3 times with complete culture medium and then were incubated for 4−24 h with mAbs, diluted in the same medium. Basal shedding of ACE was calculated 24 h after culturing with fresh "complete medium".

To determine cell-associated ACE activity as well as to quantify the rate of ACE release (by comparing the levels of ACE in the culture medium and those on the cell surface), cells from each well were lysed with 100 μL of 8 mM CHAPS. Both culture medium and cell lysates were centrifuged, and aliquots (10−50 μL) were added to 200 μL of 5 mM Hip-His-Leu or 2 mM Z-Phe-His-Leu and incubated for the appropriate time at 37 °C for the following determination of ACE activity and calculation of the rate of ACE shedding according to ref *35*.

Modeling of the N-Domain Structure. The structures of tACE, PDB 1O86 (*11*), and ACE2, PDB 1R42 (*48*), have been used for predicting the structure of the N-domain of human ACE ("closed" and "open" conformations, respectively). We have taken advantage of the 54% amino acid sequence identity (65% sequence similarity) between the N- and C-domains of human ACE and 43% amino acid sequence identity (64% sequence similarity) between the N-domain and ACE2. Sequences of the N- and C-domains of the human somatic ACE and ACE2 were aligned using Clustal X software (*49*). These sequence alignments were used as a basis for homology modeling of the N-domain structure using the Biopolymer module in the Sybyl 6.9 molecular modeling package (Sybyl 6.9 Tripos Assoc., St. Louis, MO) on the SGI Octane workstation. In the course of modeling, "in silico" mutations were performed in the amino acid se-

quences of template proteins to the sequence of the goal N-domain by the following procedure. All aligned nonidentical amino acids in the template tACE or ACE2 were mutated to the corresponding amino acids in the N-domain by changing their side chains while keeping the main chain atoms unchanged and retaining their original position in space. The most appropriate internal torsion angles in the side chains of new amino acids were chosen for each mutation site in a given secondary structure state. All insertions and deletions were handled by defining "loops", containing all amino acid residues being inserted, and several residues neighboring to positions of insertion or deletion, followed by searching the Brookhaven Protein Data Bank (*50*) for them. The conformations of the loops were considered as appropriate only when (1) the geometry of the main chain atoms neighboring to the deletion or insertion positions underwent only minimal changes and (2) no unfavorable spatial hindrance between atoms belonging to the loop and to the remaining part of the protein could be expected. Then, all proline residues and the side chains of all other amino acid residues were "fixed" by finding new appropriate values of several torsion angles so as to remove spatial overlapping between atoms. The resultant models for the N-domain were submitted to a steepest-descent energy minimization (1000 steps) using the Tripos force field. The stereochemical quality of the N-domain models was assessed by the PROCHECK program (*51*) at the same resolution as the 1O86 and 1R42 structures.

The domain movement between the "open" and "closed" conformations was analyzed using the program DynDom, available at http://www.cmp.uea.ac.uk/dyndom/main.jsp.

RESULTS

Previously we demonstrated that two mAbs (out of 8) directed to the N-domain of human ACE inhibited catalytic activity of the N-domain within somatic ACE (*25*). In a recent study, based on the species cross-reactivity of this set of mAbs to the N-domain and on their functional properties we proposed a location of the epitopes for some of the mAbs, including the epitope for inhibitory mAb 3A5 (*37*). Here we performed a more detailed study of inhibitory action of two inhibitory mAbs, 3A5 and i2H5, using fine epitope mapping and detailed kinetic analysis.

Anticatalytic Activity of mAbs 3A5 and i2H5. We studied inhibition of both truncated single N-domain of ACE and two-domain somatic ACE by these mAbs. The method of obtaining the N-domain of ACE did not influence the results, as we observed similar inhibitory activity of these mAbs toward recombinant truncated N-domain D629 and the N-domain obtained by limited proteolysis of the parent somatic ACE (data not shown).

Figure 1 (A and B) demonstrates that Z-Phe-His-Leu hydrolysis by the truncated N domain (having one active center) and by the somatic ACE (having N- and C-domain active centers) was inhibited by both mAbs 3A5 and i2H5 in a dose-dependent manner, but with different efficiencies: IC_{50} for mAb 3A5 inhibition of substrate hydrolysis by the truncated N domain (0.14 μg/mL) was significantly lower (more than 3-fold) than IC_{50} for i2H5 (0.54 μg/mL) in these experimental conditions, i.e., at pH 8.3 and 37 °C. The extent of inhibition of somatic ACE activity by both mAbs was

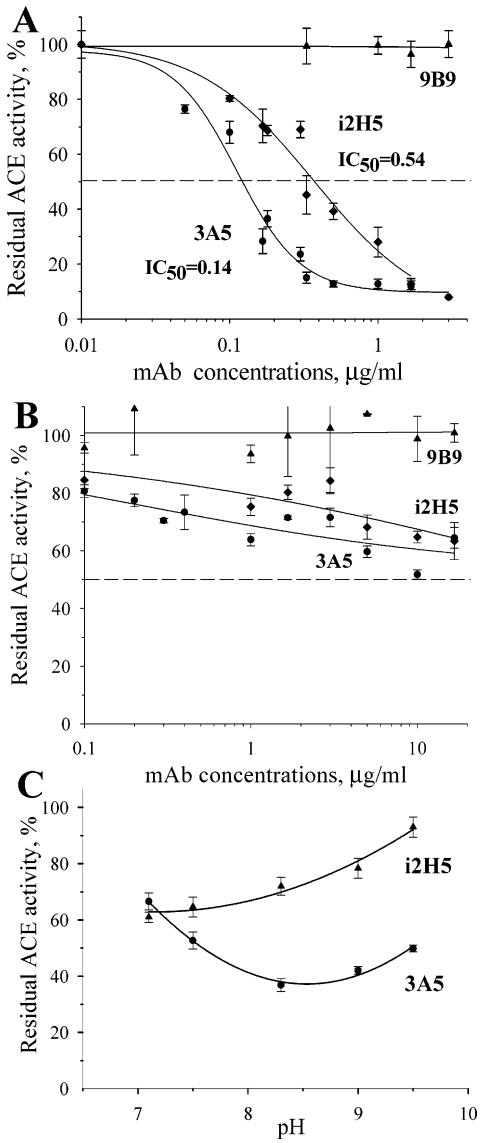

FIGURE 1: Anticatalytic effect of mAbs 3A5 and i2H5 on the Z-Phe-His-Leu hydrolysis by recombinant truncated N domain (A), wild-type somatic ACE (B), and the N-domain, obtained by limited proteolysis of the parent somatic form (C). Experimental conditions A and B: [ACE] = 10 mU/mL, 100 mM potassium phosphate buffer, containing 300 mM NaCl, 80 mM ZnSO4, pH 8.3, 37 °C. Results are shown as mean + SD of several (6−8) experiments. MAb 9B9, which does not inhibit ACE catalytic activity (*25*), was used as a negative control. C: [ACE] = 0.1 nM, [mAb] = 33 nM, 15 mM acetate−15 mM phosphate−15 mM borate buffer, containing 0.15 M KCl and 1 μM $ZnCl_2$, 25 °C. Residual ACE activity is expressed as the percentage of ACE activity remaining after mAb, 3A5 or i2H5, was added to the reaction mixture.

lower than for the N-domain, which is explained by the different substrate specificity of the whole enzyme and its domains (*22*, *25*, *27*) and by the fact that mAbs 3A5 and i2H5 are directed to the epitopes located on the N-domain (*25*). The values of IC_{50} for inhibition of single N-domain by mAb 3A5 and i2H5 when Hip-His-Leu was a substrate were similar, whereas the extent of inhibition of Hip-His-Leu hydrolysis by somatic two-domain ACE by these mAbs was significantly lower (data not shown). The reason for the substantial difference in inhibitory action of mAbs 3A5 and i2H5 on Z-Phe-His-Leu and Hip-His-Leu hydrolysis by the whole ACE molecule can be explained by the preferential

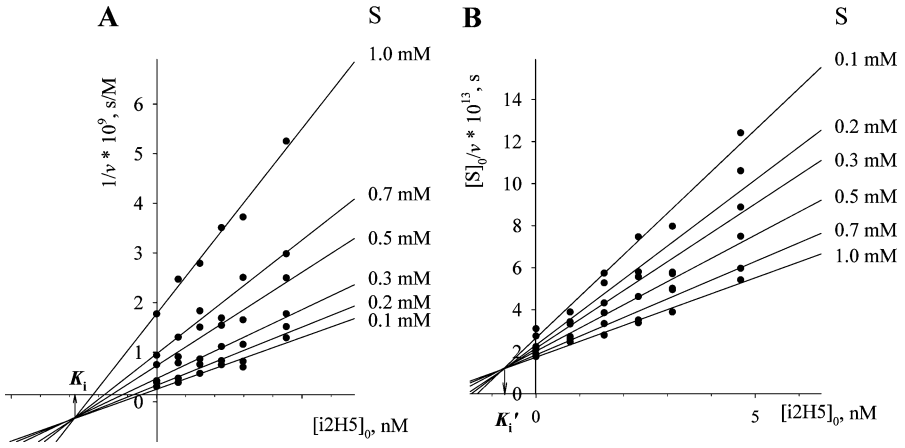

FIGURE 2: Dixon (A) and Cornish-Bowden (B) plots of N-domain inhibition by mAb i2H5. Experimental conditions: [ACE] = 0.1 nM, PBS-II buffer, 25 °C. Substrate: Z-Phe-His-Leu.

hydrolysis of the Hip-His-Leu by the C-domain at pH 8.3 (*22*, *25*).

The efficiencies of inhibition of the N-domain of ACE by both mAbs 3A5 and i2H5 are dependent, however, on the pH value of the reaction medium. Figure 1C demonstrates the pH dependence of N-domain inhibition by both mAbs at a constant ratio [ACE]/[mAb]. The mode of the function "inhibitory effect − pH" is different for the two mAbs. While inhibitory activity of mAb i2H5 decreased with pH value, the curve of the dependence of inhibitory efficiency of mAb 3A5 had an optimum near pH 8.5. Thus, the difference in the inhibitory action of these mAbs is dependent on the pH value of the medium and is the most pronounced near pH 8.5.

Kinetic Analysis of ACE Inhibition by mAbs 3A5 and i2H5. To study the anticatalytic action of mAbs 3A5 and i2H5 in more detail, we determined the kinetic mechanism of inhibition of the N-domain of ACE by the two mAbs in solution at pH 7.5. For this purpose we performed several sets of experiments; each set included measuring residual ACE activity at different mAb concentrations (more and less than the preliminarily determined IC_{50} value) at a constant concentration of the substrate Z-Phe-His-Leu. For different sets of experiments, substrate concentration varied in the range 0.1−1 mM.

In general, the rate of the enzymatic reaction in the presence of inhibiting mAbs is represented by equation

$$v = \frac{k'_{cat}[E]_0[S]_0}{[S]_0 + K'_m} \quad (5)$$

where $[E]_0$ and $[S]_0$ are initial concentrations of an enzyme and a substrate, while k'_{cat} and K'_M are the effective catalytic constant and effective Michaelis constant, respectively. These parameters depend both on the inhibitor (antibody) concentration, $[I]_0$, and on the value of the inhibition constant, K_I. Data processing in Dixon coordinates $1/v$ vs $[I]_0$ and modified Cornish-Bowden coordinates $[S]_0/v$ vs $[I]_0$ (Figure 2) allowed us to determine the kinetic mechanism of the N-domain inhibition by anticatalytic mAbs, 3A5 and i2H5, and state that this mechanism is *mixed* according to the Dixon classification (*44*) for both mAbs. This mechanism is represented by Scheme 1. According to this scheme, mAb is able to bind both with free enzyme and with the enzyme−substrate complex; however, the complex E·S·Ab is nonproductive and only the E·S complex can form a product. Thus, binding of anticatalytic mAb, 3A5 or i2H5, with the N-domain of ACE totally blocks its catalytic activity.

Scheme 1

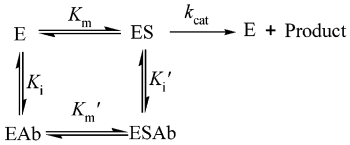

The values of the binding constant of antibodies with free enzyme, K_I, were found from intersection points of the sets of straight lines in Dixon coordinates and were equal to 2.9 ± 0.9 nM for mAb i2H5 (Figure 2A) and 4.7 ± 0.9 nM for mAb 3A5 (graph not shown). The values of the binding constants of mAbs with the enzyme−substrate complex were found from data processing in Cornish-Bowden coordinates and were equal to 0.7 ± 0.03 nM for mAb i2H5 (Figure 2B) and 0.9 ± 0.05 nM for mAb 3A5 (graph not shown). Similar results were obtained with angiotensin I as a substrate (data not shown).

Thus, according to kinetic analysis, both mAbs bind better with the enzyme−substrate complex, which, in turn, implies that upon binding of a substrate conformational adjustments in the N-domain structure occur.

In a separate experiment, similar values for the binding constant, K_{app}, were determined using the N-domain adsorbed to plastic (direct ELISA) and mAbs i2H5 and 3A5. Data processing in Scatchard coordinates gave K_{app} of 1.73 ± 0.5 nM (n = 2) and K_{app} of 2.9 ± 0.4 nM (n = 2) for mAbs i2H5 and mAb 3A5, respectively. The value of the binding constant for mAb 3A5 determined using somatic ACE adsorbed to plastic appeared to be equal to 2.6 ± 0.1 nM. Hence, the adsorption of ACE to microtiter wells did not cause any dramatic deformation in its structure, at least, in the region of its contact with mAbs i2H5 and 3A5.

Lisinopril Effect on the Antibody Binding with the N-Domain of ACE. The above-mentioned kinetic analysis indicates that mAbs i2H5 and 3A5 bind better with the N-domain of ACE in the presence of a substrate in solution. Therefore, we could expect that binding of any ligand to the ACE active site would affect mAb binding to ACE in the same manner. To prove this, we performed a series of experiments on binding of mAbs i2H5 and 3A5 to the

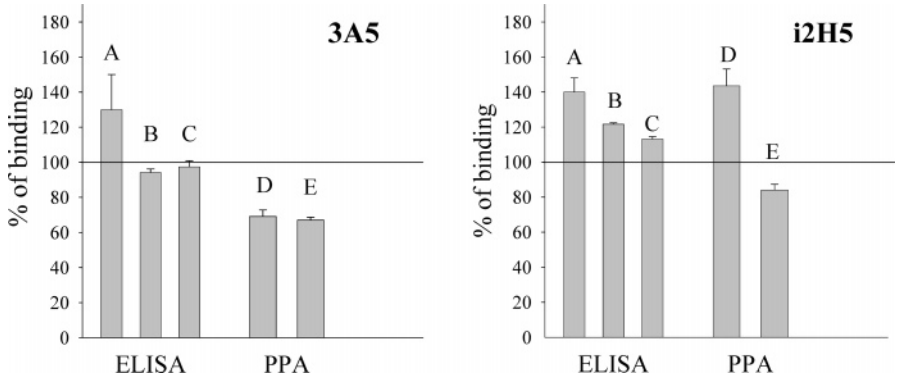

FIGURE 3: Effect of lisinopril on mAbs 3A5 and i2H5 binding with N-domain of ACE. A: Binding of mAbs to the N-domain, directly bound to microtiter plate wells. B: Precipitation of N-domain protein by mAbs, directly bound to microtiter plate wells. C: Precipitation of N-domain protein by mAbs, bound to microtiter plate wells via goat anti-mouse IgG bridge. D: Precipitation of N-domain ACE activity (with Z-Phe-His-Leu as a substrate) precipitated by mAbs, directly bound to microtiter plates. E: Precipitation of N-domain ACE activity (with Z-Phe-His-Leu as a substrate) precipitated by mAbs, bound to microtiter plates via goat anti-mouse IgG. Binding of mAbs to ACE, precipitation of ACE N-domain protein, and precipitation of the activity of the N-domain by mAbs in the absence of lisinopril were taken as 100%.

N-domain of ACE and somatic ACE in different settings in the presence of the specific ACE inhibitor, lisinopril.

MAbs binding to the N-domain, directly adsorbed to microtiter plate wells (direct ELISA), was significantly enhanced in the presence of lisinopril (Figure 3, bar A): 140 $\pm$ 8% and 130 $\pm$ 20% ($n = 3$) from control for mAbs i2H5 and 3A5, respectively. The values of the binding constant, K_{app}, for mAbs i2H5 and 3A5 with the N-domain adsorbed to the wells were estimated to be equal to 0.53 $\pm$ 0.06 nM and 0.9 $\pm$ 0.08 nM ($n = 3$), respectively, which is much the same as the values of the binding constants of these mAbs with the ACE−substrate complex determined by us in solution. The value of the binding constant for mAb 3A5 with somatic ACE adsorbed to plastic was 1.0 $\pm$ 0.1 nM.

These values, however, significantly differ from those obtained for the free enzyme, both in solution (N-domain) and on plastic (N-domain and somatic ACE).

The influence of lisinopril on the binding of mAbs 3A5 and i2H5 to the truncated N domain was studied by other two approaches as well. In one set of experiments mAbs were adsorbed to the microtiter plates coated via a goat anti-mouse IgG bridge, whereas in the second set mAbs were bound directly to uncoated plates. Precipitation of ACEs by mAbs 3A5 and i2H5 was estimated by two methods: (i) The amount of ACE protein precipitated by mAbs was quantified with sheep polyclonal antibodies to human ACE conjugated with peroxidase (*46*); (ii) Enzymatic activity precipitated by mAbs was estimated by direct measurement of ACE activity in the wells of microtiter plates by fluorimetric assay (*25*). As a negative control we used mAb 9B9, which did not show a significant inhibitory potency toward the N domain active site at least in solution.

These experiments (Figure 3) demonstrate the following:

(1) The presence of lisinopril did not affect the amount of ACE protein precipitated by mAb 3A5 bound to microtiter plates via goat anti-mouse IgG (Figure 3, mAb 3A5, bars B, C). However, binding of 3A5 with ACE complexed with lisinopril retained some inhibitor within the active center, because ACE activity precipitated by this mAb in the presence of lisinopril was significantly ($p < 0.05$) lower (Figure 3, mAb 3A5, bars D, E);

(2) Precipitation of ACE protein by mAb i2H5, bound to microtiter plates via goat anti-mouse IgG, increased slightly in the presence of lisinopril, albeit significantly: 113.5 $\pm$ 1.9% of control, $n = 3$, $p < 0.05$ (Figure 3, mAb i2H5, bar C). Precipitated ACE activity, 84.1 $\pm$ 3.2% of control, $n = 3$, $p < 0.05$ (Figure 3, mAb i2H5, bar E), did not follow the increase in precipitation of ACE protein, which indicates that binding of mAb i2H5 to the complex of ACE with inhibitor also restricts a natural dissociation of lisinopril from the active center during washing steps in this assay.

(3) Both ACE protein and ACE activity precipitated by mAb 3A5 in the presence of lisinopril were much the same regardless of how this mAb was immobilized on the microtiter plate, via goat anti-mouse bridge or directly. However, the effect of lisinopril on mAb i2H5 binding was greatly affected by the mode of mAb immobilization: precipitation of ACE protein in the presence of lisinopril by mAb i2H5 directly bound to the plastic was stronger than when mAb i2H5 was immobilized via goat-anti-mouse bridge: 121.6 $\pm$ 0.8% of control ($p < 0.05$) compared to 113.5% (Figure 3, mAb i2H5, bars B, C). ACE activity precipitated in the presence of lisinopril by mAb i2H5 directly bound to the microtiter plates was higher (143.5 $\pm$ 9.6% of control, $p < 005$) compared with only 84.1% in the case of mAb i2H5 immobilized via goat anti-mouse IgG (Figure 3, mAb i2h5, bars D and E, respectively).

These results also indicate that the greater flexibility of mAb i2H5 fixed via goat-anti-mouse bridge provided more inhibition of ACE activity by this mAb. Another fact to support a proposed effect of mAb i2h5 flexibility on the ACE inhibition is that the greatest extent of N-domain active center inhibition was observed when both ACE and mAbs were in solution, i.e., at their maximal flexibility (See Figure 1A).

In a separate experiment, we used EDTA at concentrations up to 5 mM, as an alternative inhibitor, so as to remove Zn^{2+} from the active site of ACE. We found that EDTA neither increases nor decreases the binding of mAbs 3A5 and i2H5 with both recombinant human somatic ACE and truncated N domain (data not shown).

Mutagenesis of the N-Domain of ACE. In a previous study we defined broadly the epitopes for some mAbs to the N-domain of human ACE by examining the cross-reactivity of these mAbs, raised against human ACE, with naturally occurring variants of ACE, and the differences in functional

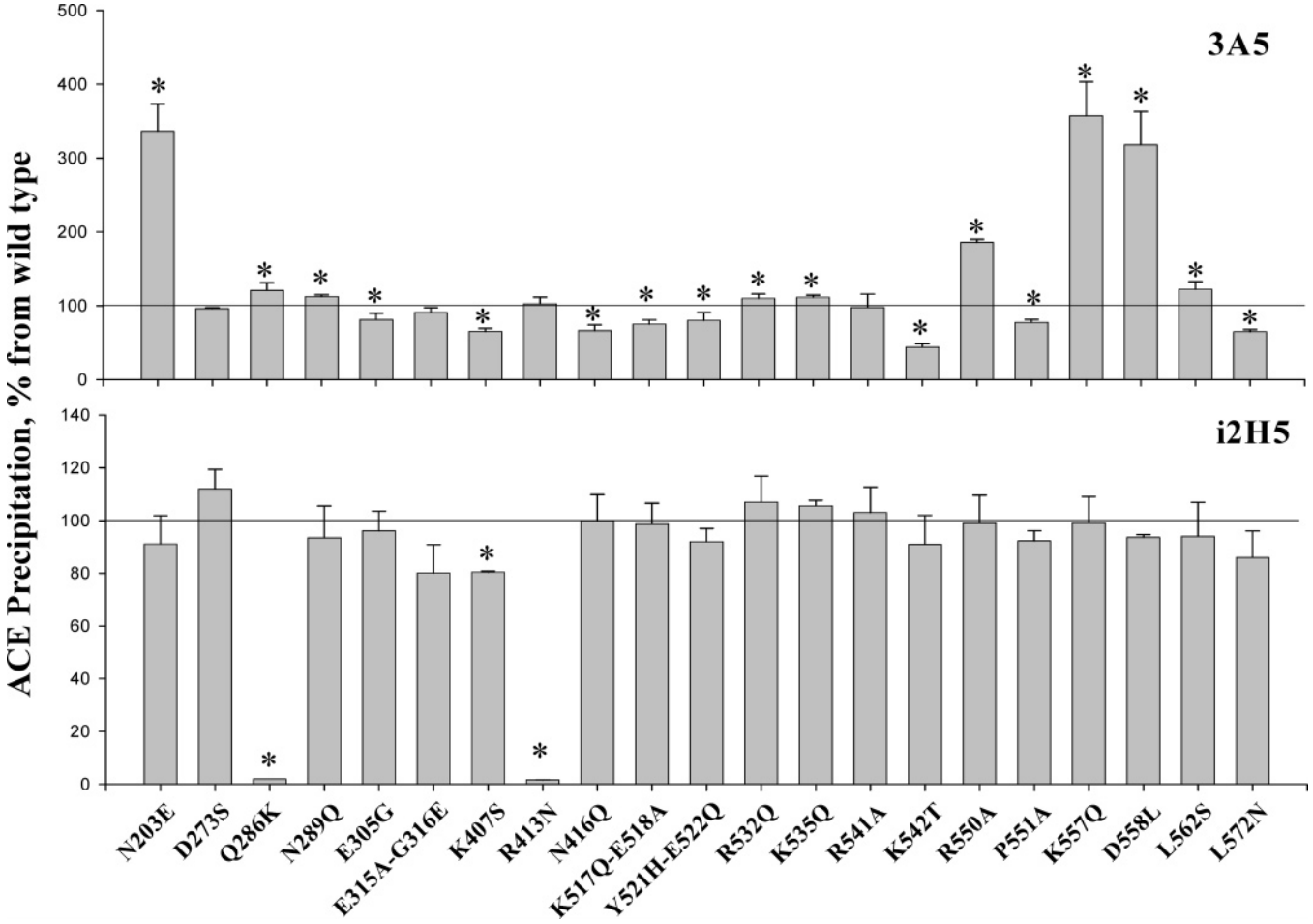

FIGURE 4: The effect of mutations on the precipitation of ACE activity by mAbs. ACE activity of culture fluid from CHO cells expressing each mutant was equalized with ACE activity of truncated N-domain (D629), which was considered here as a wild-type ACE, in a range of 5−10 mU/mL (with Z-Phe-His-Leu as a substrate). Then precipitation of ACE activity of each mutant by mAbs 3A5 and i2H5 was estimated by the plate precipitation assay. Results are expressed as a percentage of precipitated ACE activity from each mutant to that of truncated N fragment and shown as mean ± SD of 4−6 independent experiments, each in duplicate or triplicate.

properties of these mAbs (*37*). However, the residues that could be evaluated were limited by the availability of amino acid sequences of naturally occurring variants. Replacement of specific amino acids in the N-terminal domain by site-directed mutagenesis allowed for a rationally designed, systematic and quantitative analysis of the interaction between antibodies and ACE.

Figure 4 demonstrates the effect of 21 mutations in the N-terminal domain on the binding with mAbs 3A5 and i2H5. The chosen amino acid residues in the N-domain were substituted by the corresponding amino acids in the C-domain, because neither mAb 3A5 nor i2H5 recognizes C-terminal domain.

The rationale for the choice of amino acid residues to be mutated for fine epitope mapping of mAb 3A5 was dictated by the previously predicted region for the epitope 3A5, in particular, amino acid residues A564, Q568, and L572 (*37*).

The region for the mAb i2H5 epitope (and choice of amino acid residues for mutagenesis) was chosen based on the following facts:

(i) Previously we made the K407S mutation in the N-terminal domain construct (D737), and found that this mutation almost completely abolished the binding of mAb 6A12 (data not shown), which recognizes an epitope that highly overlaps with the epitope for i2H5 (*25*). Binding of another mAb, belonging to this group, 1G12, was diminished significantly after mutation as well.

(ii) Binding of all mAbs belonging to this group (i2H5, 1G12, and 6A12) was completely absent with chimpanzee ACE (*52*), which has a substitution in the same region: E403A and R413N (*53*).

Thus, we chose for mutagenesis those amino acid residues that fall into the region and within an area of <700−800 Å^2: the mean value of the surface area of the epitopes for mAbs (*54*, *55*) around amino acid residues already known as counterparts of the epitope recognized by a definite mAb. Some amino acid residues were chosen on the basis of analysis of the N-domain model, described below. They are predominantly "hills" on the protein surface, as this would make them most favorable for interacting with antibody. We considered the effect of mutation as positive only when a change of 10%, or more, occurred in the binding of mutated ACE with mAb.

Anticatalytic Activity of mAbs 3A5 and i2H5 on the N-Domain Mutants. The 21 mutants can be classified into three subsets with respect to their effects on ACE precipitation by mAb 3A5: (1) those mutants where precipitation of ACE activity by mAb 3A5 did not change in comparison with wild-type ACE (in that case D629)—E315A−G316E, R413N, and R541A; (2) those mutants where precipitation

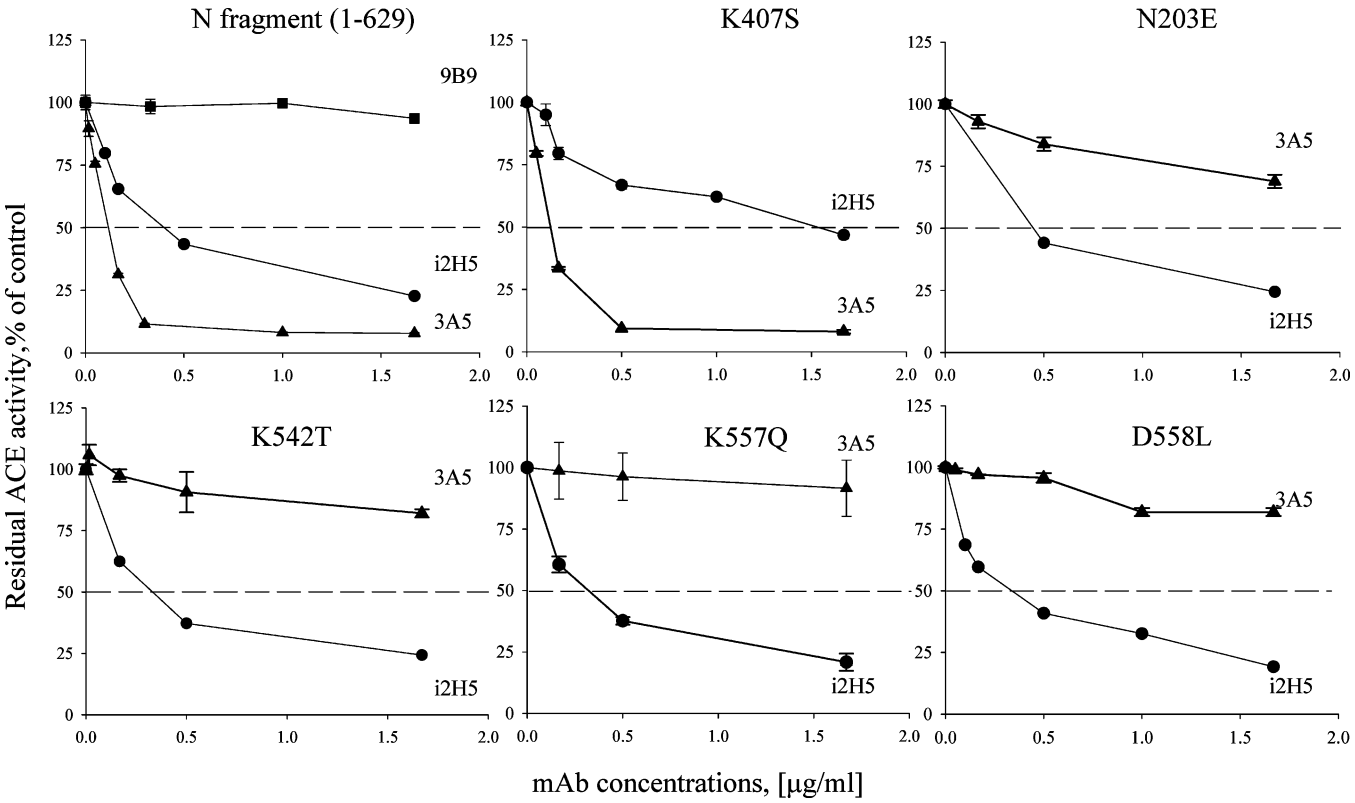

FIGURE 5: Anticatalytic effect of mAbs 3A5 and i2H5 on N domain mutants. Assay conditions were as described in Materials and Methods and in the caption to Figure 1. Residual ACE activity is expressed as the percentage of ACE activity remaining after mAb 3A5 or i2H5 was added to the reaction mixture in comparison with ACE activity in the presence of normal, nonimmune mouse IgG, which was taken as 100%. MAb 9B9, which did not inhibit ACE catalytic activity (*25*), was used as negative control for the truncated N-domain, which was considered here as a wild-type ACE. The effect of mAb 9B9 on the catalytic activity of other mutants was absent and is not shown for clarity. Results are shown as mean ± SD of 3−4 experiments, each in duplicate.

of ACE activity by mAb 3A5 decreased in comparison with wild type—most of the studied mutants; (3) those mutants where precipitation of ACE activity by mAb 3A5 increased in comparison with wild type—N203E, R550A, K557Q, and D558L.

Of particular interest were the mutants belonging to the third group. Because mAb 3A5 effectively inhibits the catalytic activity of the truncated N-terminal domain (D629) (see Figure 1), the increase in the precipitation of ACE activity by mAbs immobilized on microtiter plates might be due to a dramatic increase (2−3-fold) in affinity of mAb 3A5 binding with these mutants or to an abolition of the anticatalytic properties of this antibody.

In order to define the reason for the increase in precipitation of ACE activity we determined the anticatalytic effect of mAbs 3A5 and i2H5 on the N domain mutants in solution.

Figure 5 demonstrates the effect of mAbs 3A5 and i2H5 on the catalytic activity of mutants representing a spectrum of the responses. One can see that the K407S mutation, which led to a significant albeit weak decrease in the precipitation of ACE activity by mAb i2H5 (Figure 4), also showed a significant decrease of mAb i2H5 inhibitory potency: IC_{50} increased more than 3-fold (Figure 5). K542T mutation, in which ACE activity precipitation by mAb 3A5 was significantly decreased (more than 2-fold: Figure 4), also demonstrated a dramatic decrease in anticatalytic activity (Figure 5). Mutations Q286K and R413N, whose effects on the precipitation of ACE activity by mAb i2H5 were dramatic—>90% decrease (Figure 4)—completely abolished the inhibitory potencies of mAb i2H5 as well (not shown). Other mutants demonstrating a decrease in ACE precipitation by mAb 3A5 in the plate precipitation assay (Figure 4) also showed a significant and corresponding decrease in the anticatalytic potency of mAb 3A5 (not shown).

In contrast, all four mutants, where precipitation of ACE activity by mAb 3A5 was dramatically increased—N203E, K557Q, D558L, and R550A (Figure 4)—demonstrated a remarkable decrease in the anticatalytic effect of mAb 3A5 (Figure 5). The effect of R550A on 3A5 inhibition, the same as for three other mentioned mutations, is not shown. Therefore, the dramatic increase in precipitation of ACE activity by mAb 3A5 obtained with these mutants should be attributed not to better binding of mAb 3A5 but to abolition of its anticatalytic potency toward mutants with critical amino acid substitutions N203E, R550A, K557Q, and D558L.

In most mutants, where binding of one mAb was changed, the binding of another mAb was not influenced, confirming that the epitopes for mAbs 3A5 and i2H5 are essentially nonoverlapping (*25*).

Modeling of the N-Domain of ACE and Fine Epitope Mapping. Crystallization of the C-domain of human ACE (tACE) and resolution of its 3D structure (*11*) made possible the modeling of the N-domain of human ACE as well (*26*, *33*, *37*). By combining knowledge of the 3D structure of the N-domain and the effects of site-directed mutagenesis we became able to define epitope mapping of mAbs 3A5 and i2H5 in fine detail.

Kinetic analysis together with direct ELISA and activity precipitation experiments demonstrate different affinities of

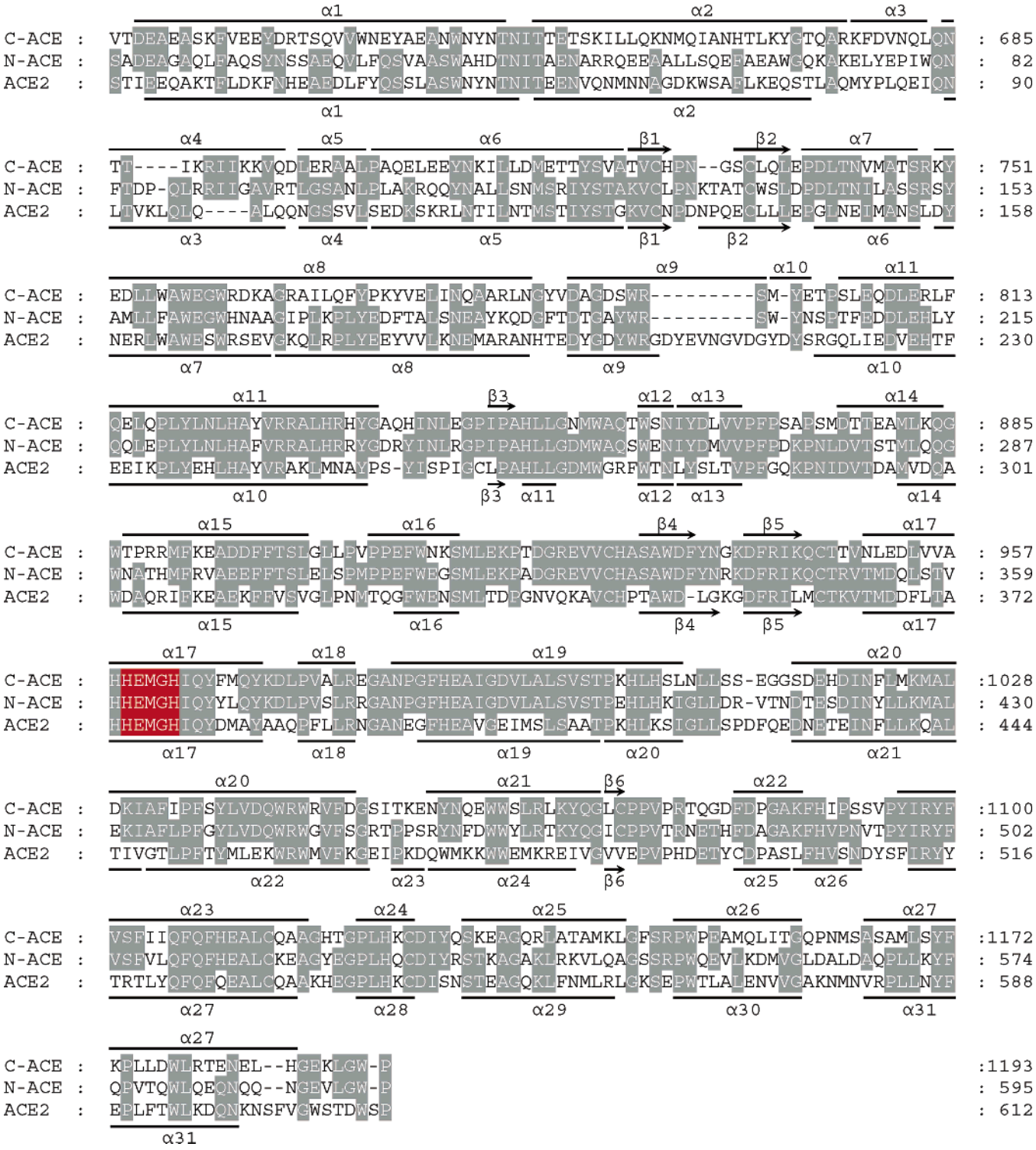

FIGURE 6: Sequence alignment of the ACE N-domain with C-domain and ACE2. Identical residues between the N- and C-domains and between the N-domain and ACE2 are shown against a background. Secondary structure elements (α-helices and *β*-strands) are represented on the top of the alignment according to the resolved tACE and ACE2 crystal structures. Zinc binding motif is marked by red. The numbering of ACE relates to mature somatic ACE (*8*).

mAbs 3A5 and i2H5 for the free and ligand-bound N-domain of ACE indicating, therefore, the possible existence of two conformational states for this domain. The native C-domain structure was reported to be nearly identical to the inhibitor-bound C-domain structure (*11*), suggesting that no ligand-dependent conformational change occurs for the C-domain. However, the reported C-domain structure actually appeared to contain two ligands, acetate and *N*-carboxyalanine, that are bound to the active site of the enzyme, and, therefore, might represent another ligand-bound structure. For this reason we employed two models of the N-domain of ACE: the "closed" conformation was based on the structure of the C-domain of human ACE (PDB 1O86), while the "open" conformation was based on the structure of human ACE-related carboxypeptidase, ACE2 (PDB 1R42).

The aligned sequences of the N-domain, the C-domain, and ACE2 are presented in Figure 6. There are two gaps with a total of five inserted amino acids and 272 differences

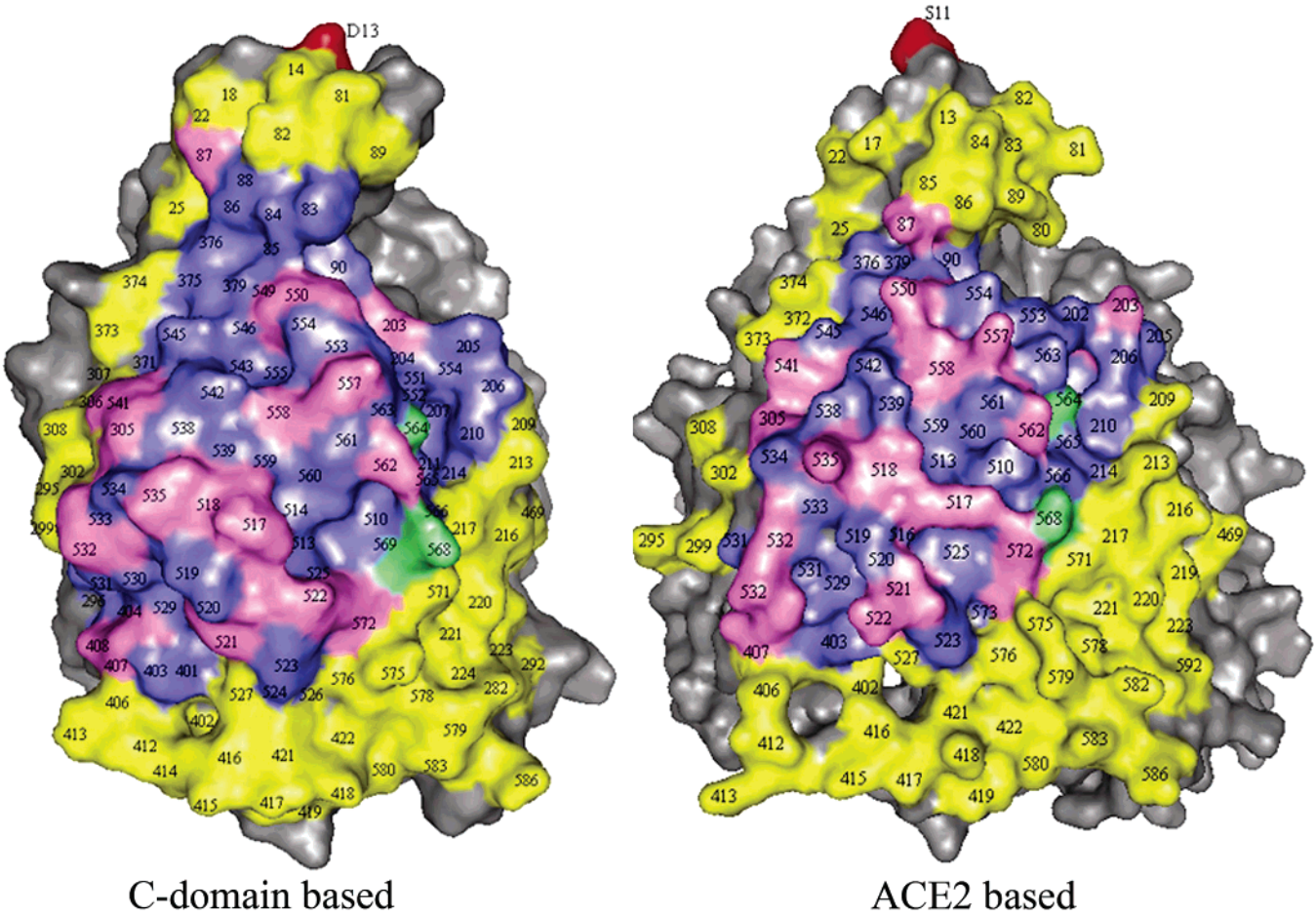

FIGURE 7: Fine epitope mapping for mAb 3A5 (surface presentation). The structure of the N-domain of human ACE was modeled based on the 3D structures of human C-domain (PDB 108A) and ACE2 (PDB 1R42).The various amino acid residues belonging to the epitope for mAb 3A5 are color-coded. Amino acid residues, whose substitution results in significant changes in mAb 3A5 binding, are marked by purple. Amino acid residues marked by green were recently predicted as belonging to the epitope for mAb 3A5 (*37*). Amino acid residues marked by blue were suggested to be in the epitope for mAb 3A5 because (i) they are located between amino acid residues crucial for mAb 3A5 binding and (ii) the surface of the epitope for the mAb should be about 500−900 Å^2 (*54*, *55*). Amino acid residues around the putative epitope for mAb 3A5 were marked by yellow for orientation. The rest of the surface is in gray. The first amino acid residues seen in the modeled N-domain structures are colored in red.

between the N- and C-domains over the 595 aligned residues, which correspond to 54% of sequence identity. There are, however, five deletions and 3 insertions with total 21 deleted/inserted amino acid residues within 340 differences between the N-domain and ACE2 (43% of sequence identity). A higher conservation of amino acid residues in ACE2, C-domain and N-domain structures is observed in the sequence 200−550 (numeration according to the N-domain). The central sequence containing and surrounding the HEMGH motif is most conservative.

The secondary structure elements described for the templates (tACE and ACE2) are mapped in the alignment (Figure 6). The main elements of the secondary structures of the template proteins coincide well providing feasible comparison of the two models of the N-domain. The region D85−A94 in the N-domain, however, contains both deletion and insertion in the template α-helices. This could be the reason for some inexactitude in modeling of this particular region.

Analysis of the Ramachandran plots using the program PROCHECK (*51*) for both N-domain models showed 82% and 77% of the residues in the N-domain structures modeled with the C-domain and ACE2 as templates, respectively, in the most favorable region.

Fine epitope mapping of mAb 3A5 and i2H5 is presented in Figure 7 and Figure 8, respectively, using both N-domain model structures. Both "open" and "closed" N-domain conformations exhibit similar relative dispositions of α-helixes and amino acid residues within the epitopes for binding mAbs 3A5 and i2H5.

The surface area of the epitope for mAb 3A5 was estimated to be about 740 Å^2. This area is slightly longer on the surface of the "open" structure of the N-domain than on the "closed" structure, e.g., amino acid residues N203 and L562 are 19.16 Å and 18.69 Å from each other in the "open" and "closed" structures, respectively. Most of the amino acid residues that are counterparts of the epitope for mAb 3A5 are charged residues (50%), such as 3 Arg, 7 Lys, 4 Tyr, 6 Glu, 5 Asp, while hydrophobic amino acid residues represent only near 7% (Figure 7).

The surface area of the amino acid residues that take part in binding to antibody i2H5 was assigned at least 350 Å^2 (Figure 8). Charged amino acid residues (1 Arg, 2 Lys, 2 His, 3 Glu, 6 Asp) account for 38% of amino residues in this epitope area, while hydrophobic residues represent 25%. We propose that the real surface area of the epitope for i2H5 is much larger, because the minimal surface for published

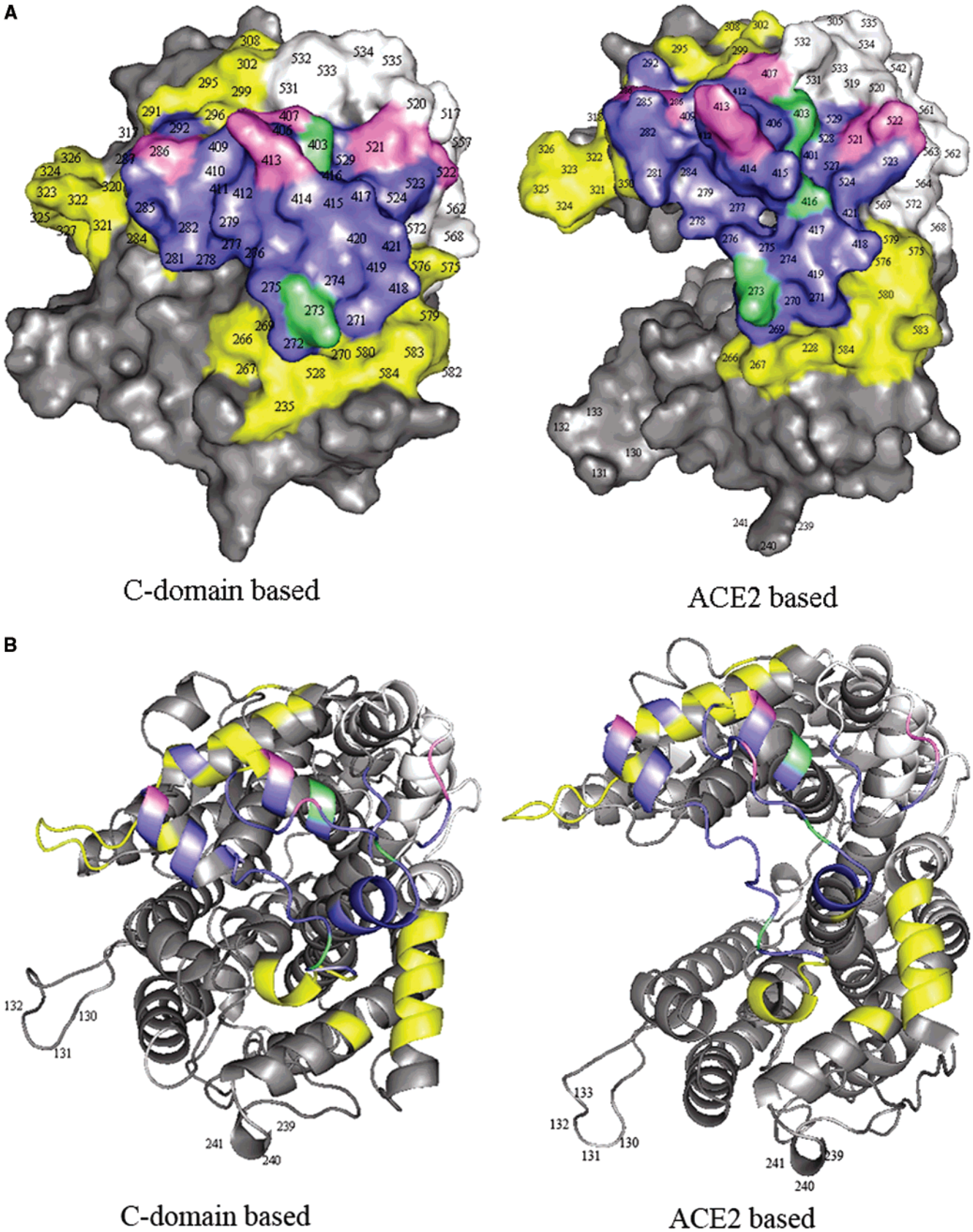

FIGURE 8: Fine epitope mapping for mAb i2H5 (surface (A) and ribbon (B) presentations). The surface and ribbon presentations of the N-domain of human ACE were modeled on the basis of the 3D structures of human C-domain (PDB 108A) and ACE2 (PDB 1R42). Various amino acid residues belonging to the epitope for mAb i2H5 are color-coded. Amino acid residues whose substitution results in significant changes in mAb i2H5 binding are purple. Amino acid residues in green were recently predicted as belonging to the epitope for mAb i2H5 (*52*). Amino acid residues in blue were suggested to be in the epitope for mAb i2H5 because (i) they are located between amino acid residues crucial for mAb i2H5 binding and (ii) the minimal surface area of the epitope for mAb is about 500 Å^2. Amino acid residues around the putative epitope for mAb i2H5 are in yellow for orientation. Residues in white belong to the epitope for mAb 3A5. The rest of the surface is in gray.

epitopes is about is 500 Å^2 (*54*, *55*). It is worth noting that the epitope for mAb i2H5 is positioned in the region of a "chewing muscle" in the jaws of the "open" structure, while in the "closed" structure it is located near one of the entrances to the active site channel (Figure 8).

The regions of epitopes for mAbs i2H5 and 3A5 are partly overlapping. This partial overlap allows binding of mAb 3A5 with the ACE−mAb i2H5 complex, whereas binding of mAb i2H5 with the ACE−mAb 3A5 complex is impossible (*25*). This could be explained by serious conformational changes in ACE structure upon binding mAb 3A5.

3A5-Induced Shedding of ACE from the Cell Surface. Previously we demonstrated that binding of mAb 3A5 to somatic ACE on the cell surface led to a dramatic increase (3−4-fold) in ACE proteolytic cleavage from the cell surface − antibody-induced ACE shedding (*35*). We suggested that binding of mAb 3A5 induced a significant conformation change in the ACE molecule on the cell surface, improved the accessibility of ACE for secretase, and, as a result, led to increased ACE shedding (*35*−*37*). It is logical to suggest that binding of mAb 3A5 with residues 203, 550, 557, 558 might determine (to some extent) the significant ACE conformational changes observed on mAb binding.

In order to investigate the role of these amino acids in the 3A5-induced ACE shedding, we generated D558L in the somatic ACE and determined its effect on binding of anti-ACE mAbs to this two-domain enzyme, as well as on 3A5-induced ACE shedding (Figure 9). As is apparent, the binding of mAb 3A5 (Figure 4), as well as mAbs i1A8 and 3G8 (data not shown), to D558L is significantly decreased as revealed by the plate precipitation assay. We also compared the rate of shedding of wild-type somatic ACE and D558L mutant under identical conditions and found that the mutation almost completely abolished 3A5-induced ACE shedding from the cell surface (Figure 9D). The basal rate of ACE shedding (without any inhibitors or mAbs) was not changed as a result of this mutation (not shown). Interestingly, despite the fact that D558L has significantly (albeit weakly) lower mAb 3G8 binding, the inhibitory effect of 3G8 on ACE shedding (*35*−*37*) was not diminished as demonstrated for the NdelACE chimeric mutant (*37*). Therefore, we suggest that covering of some critical amino acid residues on the surface of the N-domain of ACE by mAb 3A5 leads to significant changes in ACE conformation, which, in turn, leads to allosteric inhibition of ACE activity and/or determines the strong effect of mAb 3A5 on ACE shedding.

DISCUSSION

Monoclonal antibodies to ACE are extremely useful tools for investigation of enzyme functions, its structural topography, etc. Thus, mAbs to human ACE that recognize conformational epitopes on the N-domain surface and sequential epitopes on the denatured C-domain have been successfully used (i) for ACE quantification both in solution by ELISA (*46*) and on the cell surface by flow cytometry (*56*); (ii) to study the structure and function of ACE (*25*, *35*−*37*); (iii) to deliver enzymes and genes to the pulmonary endothelium (*57*−*60*); (iv) as a diagnostic tool for lung vessel visualization (*61*, *62*); and (v) for immunohistochemistry of ACE (*40*, *63*−*67*).

In this work we performed fine epitope mapping for two monoclonal antibodies to human ACE, 3A5 and i2H5, and studied the influence of these mAbs on enzyme catalysis. It was shown previously (*25*) that mAbs 3A5 and i2H5 are produced to the N-domain of human ACE and both exhibit anticatalytic activity. Measurement of the residual ACE activity at different mAb concentrations demonstrated that, in general, mAb 3A5 inhibits the N-domain of ACE more effectively than mAb i2H5 in the pH range 7.1−9.5. However, the relative efficiency of inhibition by the two mAbs is dependent on pH, because the anticatalytic effectiveness of mAb i2H5 decreases with pH, while the inhibitory activity of mAb 3A5 has an optimum near pH 8.5.

For fine epitope mapping of binding of mAbs i2H5 and 3A5, we used two N-domain models based on recently published structures of the homologous C-domain of human ACE (*11*) and the homologous ACE-related carboxypeptidase, ACE2 (*48*). Besides, we already identified at least three amino acid residues that participate in binding with mAb 3A5, namely A564, N568, and K572 (*37*). An extensive search of amino acid residues as counterparts of epitopes for both mAbs demonstrated that epitopes for mAb 3A5 and mAb i2H5 contain 50% and 38% of charged amino acid residues, respectively, whereas hydrophobic amino acid residues represent less than 25%. Taking into account the pK_a values for each amino acid residue, the overall pK_a value of the epitope for mAb 3A5 should be slightly more than 7, while the overall pK_a value of the region of the epitope for mAb i2H5 is less than 7. These results are in agreement with the dependence of the anticatalytic activity of both mAbs on pH (Figure 1C).

The areas of the epitopes for mAb 3A5 and mAb i2H5 are slightly overlapping (see Figure 8). Amino acid residues Y521, E522, G523, P524, D529, K407, and E403 are present in both epitopes. This distribution allows binding of mAb 3A5 to the ACE−i2H5 complex (*25*), though less effectively than to free enzyme. However, binding of another mAb, i2H5, to the complex ACE−3A5 was impossible (*25*). The most likely reason for this could be significant conformational changes of ACE upon binding of mAb 3A5, but not mAb i2H5.

Modeling of the structure of the N-domain of human ACE using the C-domain structure as a template resulted in a protein structure with a channel, containing the active site on one of the walls (Figure 8, see also Figures 7 and 8 in ref *37*). The ligands, substrates or inhibitors, are supposed to enter to the entrance of this channel to reach the active site (*11*, *31*). However, the authors already pointed out that the aperture of the channel opening is approximately 3 Å in diameter, too small for most peptide substrates (for example, the distance between C atoms in the benzyl ring of phenylalanine, which is a common component of ACE substrates, can reach 4.3 Å). Clearly, the C-domain of ACE must undergo some conformational change, possibly associated with its unique chloride ion activation, for the substrate to enter the channel (*68*). Thus, in the native, flexible ACE the size of the entrance to the channel should be bigger than that presented in the structure of the crystalline enzyme (*11*, *30*) in order to provide binding of a ligand.

Epitope mapping for mAb i2H5 demonstrates that it binds in close proximity to one of the entrances into the channel (Figure 8). Therefore, the anticatalytic action of mAb i2H5 could be due to direct blockade of the entrance, thus

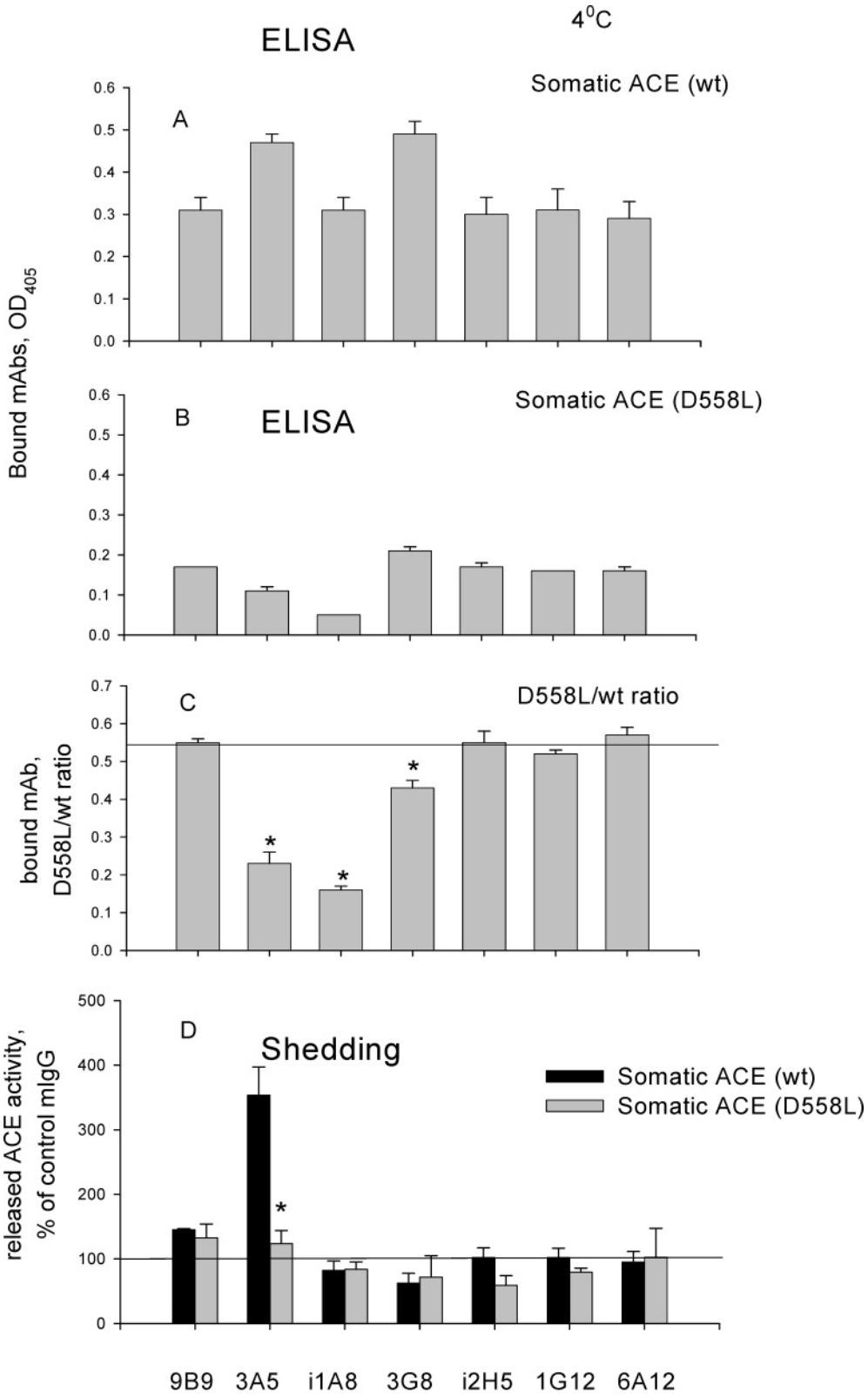

FIGURE 9: Effect of D558L mutation in somatic ACE on antibody-induced ACE shedding. A, B: Anti-ACE mAb binding (ELISA). The CHO-somatic ACE (clone 2C2) and D558L mutant were grown on 96-well plates until confluence. Anti-ACE mAbs (10 μg/mL) were added to the cells in serum-free medium (containing 2% BSA) and incubated for 2 h at 4 °C for mAb binding assay. Bound anti-ACE mAbs were revealed with goat anti-mouse IgG-alkaline phosphatase. C: The ratio D558L/wild-type of ACE binding with each mAb. (*) $p < 0.05$ for the differences of mAbs binding ratio to mutant and wild-type somatic ACE. D: The rate of antibody-induced ACE shedding. The CHO-ACE cell lines were grown on 96-well plates until confluence. Anti-ACE mAbs (10 μg/mL) were added to the cells in serum-free medium and incubated for 4 h at 37 °C for ACE shedding assay. The ACE activity shed from the plasma membrane of cells was measured fluorimetrically in a culture fluid with Hip-His-Leu as a substrate. The rate of ACE shedding was calculated as described in Materials and Methods. Antibody-induced shedding is expressed as percentage of the basal shedding of ACE (in the presence of control mouse IgG only). The data represent results of several independent experiments and are expressed as mean ± SD. (*) $p < 0.05$ for the differences of antibody-induced and basal shedding.

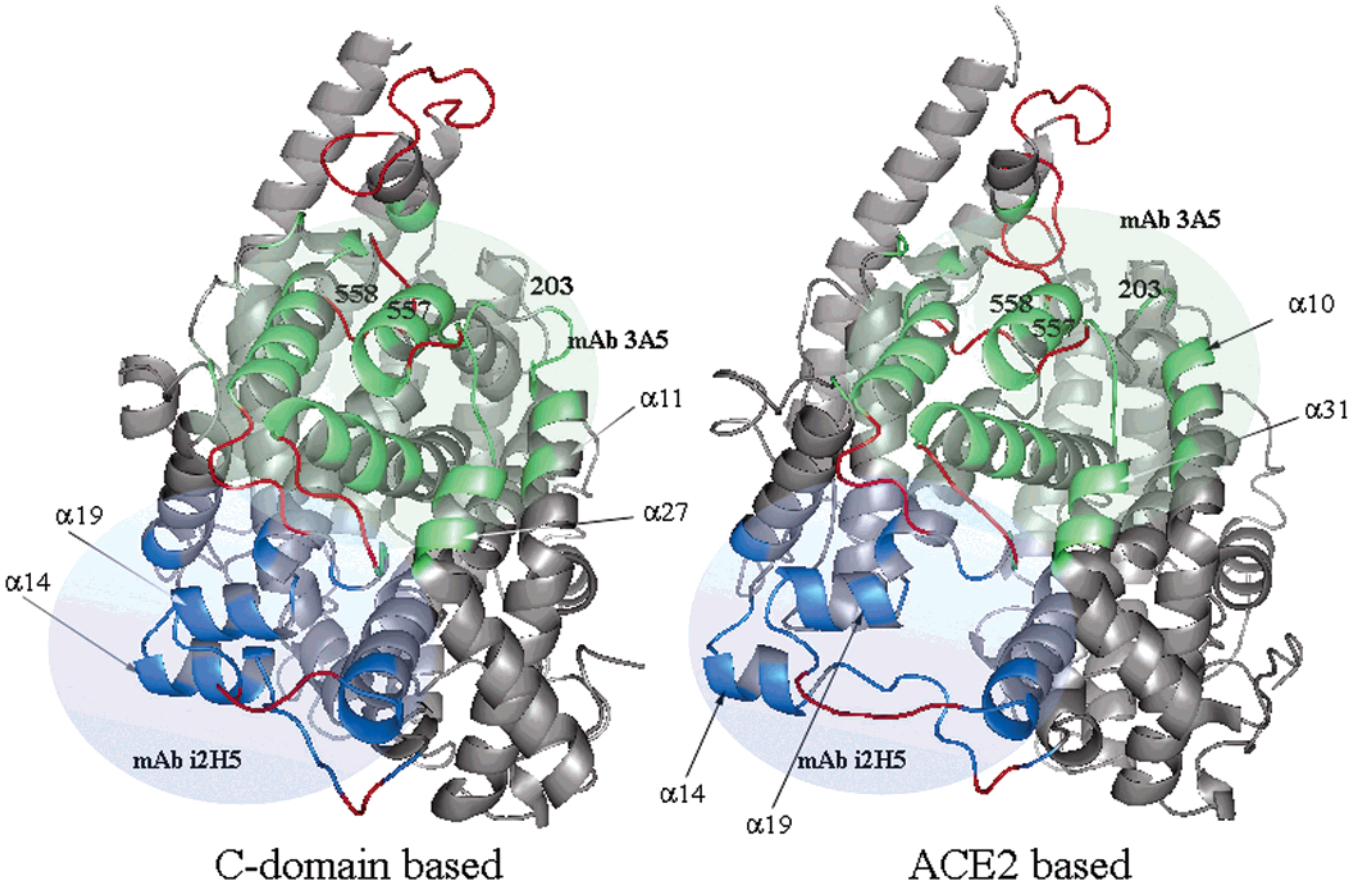

FIGURE 10: Shifting regions in the ACE N-domain upon putative hinge-bending movement (ribbon presentation). The ribbon presentation of the N-domain of human ACE was modeled on the basis of the 3D structures of human C-domain (PDB 108A) and ACE2 (PDB 1R42). The domain movement between the "open" and "closed" conformations was analyzed using the DynDom program. Amino acid residues changing spatial angles and their position concerning other elements of the molecule structure upon the hinge-bending movement are marked by red. The α-helices changing relative spatial positions are numbered. The regions of the epitopes for mAbs i2H5 and 3A5 are in blue and green colors, respectively.

obviating penetration of substrate into the active site channel. This physical mechanism of action would correspond to a noncompetitive kinetic mechanism of inhibition of ACE activity by this mAb, i.e., the mAb would be equally able to bind to the free enzyme and the enzyme−substrate complex. However, in kinetic experiments we observed a *mixed* type of inhibition, close to *uncompetitive* (a mechanism in which inhibitor binds only to an enzyme−substrate complex, but not to free enzyme), with much better binding of antibody to the enzyme−substrate complex. We obtained similar results when using lisinopril as a ligand and measuring the binding of mAb by ELISA. In this case, the presence of lisinopril caused an increase in binding of mAb i2H5 by 40% (Figure 3). The results of both kinetic experiments in solution and ELISA on the microtiter plates indicate probable conformational changes in the N-domain globule caused by a ligand binding in the active site of the enzyme and resulted in better binding of mAb i2H5 with its surface.

Epitope mapping for mAb 3A5 demonstrated that this area is quite far from both entrances to the active site channel (Figure 7). Nevertheless, in this case, we also observed a *mixed* type of inhibition of the activity of the N-domain by this mAb in solution with better binding of the mAb to the enzyme−substrate complex. The presence of inhibitor lisinopril led to an increase in binding of antibody to the N-domain by up to 30% as well (ELISA).

An investigation of the recently found structural homologue of ACE, carboxypeptidase ACE2, demonstrated that binding of a ligand to the ACE2 active site is accompanied by a so-called "hinge-bending" movement (*48*). The structure of the free enzyme represents an "open" conformation of the protein with the active site on the bottom of the "opened mouth". Binding of a ligand to the active site causes structural movements in the enzyme, which, in turn, cause "closing" of the "mouth" with the active site inside. The authors suggested that this mechanism could be common for both ACE2 and ACE (*48*). This suggestion is supported by the fact that while the 3D structure of the C-domain of human ACE was reported to be identical with inhibitor-bound structure (*11*), the first structure included two ligands, acetate and carboxyalanine, in the active site. Therefore, the structure of the C-domain cannot be considered as, in fact, free. Besides, the same hinge-bending movement has been observed for two other structural homologues of ACE and ACE2, namely, neurolysin and human thimet oligopeptidase (*69*, *70*). Most probably, this mechanism pertains to two other ACE homologues as well: *Escherichia coli* dipeptidyl carboxypeptidase Dcp has been presented in a "closed" conformation in complex with two dipeptides (*71*), and carboxypeptidase from *Pyrococcus furiosus* has been presented in an "open" conformation (*72*). On the other hand, investigation of the structure of AnCE, the *Drosophila*

homologue of ACE (*73*), showed that the structures of the free and inhibitor-bound enzyme are identical. However, the authors also pointed out that the diameters of the entrances into the active site channel (3 Å) are too small for allowing a substrate to pass through, which, in turn, suggests that conformational movements must occur on binding a ligand. Also, the 2.4 Å refinement used in this work may be not enough for discovery of a small ligand in the active site (similar to ligands in the ACE structure).

Thus, conformational changes connected with a ligand binding in an enzyme active site, or a hinge-bending movement, could be a common mechanism for all these structurally related zinc-dependent enzymes. Moreover, the possibility exists that these enzymes have a common ancestor protein (*74*).

This suggestion allows us to explain the results obtained with the N-domain of ACE and anticatalytic mAbs i2H5 and 3A5. Epitope mapping for mAb i2H5 shows that the amino acid residues included in this epitope are located on the sides of the "mouth" with the active site inside (Figure 8), and, therefore, the "closed" conformation appears preferable for this mAb binding. If the N-domain of ACE could exist in both "closed" and "open" conformations, binding of a ligand (substrate or inhibitor) in the active site would cause the "jaws" closing and increase mAb i2H5 binding to the N-domain. The inhibiting action of mAb i2H5 itself could consist of fixing of one of the conformations of the ACE molecule, thus preventing movement of the enzyme and, therefore, catalysis.

The mechanism of inhibition of ACE activity by mAb 3A5 can be also explained by fixing one of the ACE conformations upon binding. The epitope for mAb 3A5 is located on three α-helixes, which move relative to each other upon changing from the "open" to the "closed" conformation (Figure 7). Thus, binding of this mAb can fix the relative position of these structural elements and, therefore, prevent catalysis. This suggestion is supported by the fact that mutation of amino acid residues, N203, R550, K557, and D558, positioned on these three α-helixes (Figure 7) does not disturb binding of mAb 3A5 due to multipoint interactions of the mAb with ACE, but abolishes its inhibitory action toward ACE.

Moreover, both epitopes for mAbs i2H5 and 3A5 contain amino acid residues and structural elements that could be directly involved in the hinge-bending movement, as can be seen in Figure 10. Thus, the epitope for mAb i2H5 contains P272, D273, and amino acid residues in positions 412−416; the epitope for 3A5 includes R381, G382, A383, R550, P551, G561, L562, and amino acid residues in positions 529−533; both epitopes contain the amino acid residues 520−523. These amino acid residues are marked by red in Figure 10. During the movement of ACE from an "open" conformation to a "closed" conformation, the positions of these residues relative to other elements of the molecular structure are changing. The torsion angles of these residues, as revealed by the DynDom program, are different in the two N-domain conformations as well. Moreover, relative spatial positions of some secondary structural elements also appeared to be different in the "closed" and "open" conformations of the N-domain: (i) the positions of α-helices α14 and α19 in the mAb i2H5 epitope differ in the two N-domain structures; (ii) the positions of α-helices α11 and α27 in the mAb 3A5 epitope in the N-domain structure with the C-domain as a template and the positions of corresponding α-helices α10 and α31 in the N-domain structure with ACE2 as a template differ as well (Figure 10).

The results of the present study also demonstrate that the amino acid residue D558 (and, likely, N203, R550, and K557) in the epitope for mAb 3A5, crucial for its inhibitory action, is also crucial for the significant increase in ACE shedding after binding with mAb 3A5 (Figure 9), thus confirming our previous suggestion (*36*, *37*) that the conformational changes in the ACE molecule upon mAb 3A5 binding are responsible for both effects of this mAb: anticatalytic activity and antibody-induced shedding from the cell surface.

Thus, fine epitope mapping of anticatalytic mAbs in conjunction with a homology model of ACE N-domain structure has allowed us to reveal putative mechanisms of inhibitory action of mAbs 3A5 and i2H5 and shed some light on the mechanism of angiotensin-converting enzyme function.

ACKNOWLEDGMENT

We are grateful to Prof. J. Riordan (Harvard Medical School) for the critical reading of the manuscript and to Pierre Redelinghuys (University of Cape Town, South Africa) for technical advice and providing two mutants of the N-domain: N289Q and N416Q.

REFERENCES

1. Ehlers, M. R. W., and Riordan, J. F. (1989) Angiotensin-converting enzyme: new concepts concerning its biological role, *Biochemistry 28*, 5311−5318.
2. Skidgel, R. A., and Erdos, E. G. (1993) Biochemistry of angiotensin I- converting enzyme, in *The Renin-Angiotensin System* (Robertson, J. I. S., Nichols, M. G., Eds.) pp 10.1−10.10, Glower Medical Publishing, New York.
3. Corvol, P., Eyries, M., and Soubrier, F. (2004) Peptidyl-dipeptidase A/Angiotensin I-converting enzyme, in: *Handbook of Proteolytic Enzymes* (Barret, A. A., Rawlings, N. D., Woessner, J. F, Eds.) pp 332−349, Elsevier Academic Press, New York.
4. Dzau, V. J., Bernstein, K., Celermajer, D., Cohen, J., Dahlof, B., Deanfield, J., Diez, J., Drexler, H., Ferrari, R., van Gilst, W., Hansson, L., Hornig, B., Husain, A., Johnston, C., Lazar, H., Lonn, E., Luscher, T., Mancini, J., Mimran, A., Pepine, C., Rabelink, T., Remme, W., Ruilope, L., Ruzicka, M., Schunkert, H., Swedberg, K., Unger, T., Vaughan, D., and Weber, M. (2001) The relevance of tissue angiotensin-converting enzyme: manifestations in mechanistic and endpoint data, *Am. J. Cardiol. 88* (Suppl.), 1L−20L.
5. Danilov, S. M., Franke, F. E., and Erdos, E. G. (1997) Angiotensin-Converting Enzyme (CD143), in *Leucocyte Typing VI: White Cell Differentiation Antigens* (Kishimoto, T., et al., Eds.) pp 746−749, Garland Publishing Inc., New York.
6. Franke, F. E., Metzger, R., Bohle, R.-M., Kerkman, L., Alhenc-Gelas, F., and Danilov, S. M. (1997). Angiotensin I-Converting Enzyme (CD 143) on endothelial cells in normal and in pathological conditions, in *Leucocyte Typing VI: White Cell Differentiation Antigens* (Kishimoto, T., et al., Eds.) pp 749−751, Garland Publishing Inc., New York.
7. Hagaman, J. R., Moyer, J. S., Bachman, E. S., Sibony, M., Magyar, P. L., Welch, J. E., Smithies, O., Krege, J. H., and O'Brien, D. A. (1998) Angiotensin-converting enzyme and male fertility, *Proc Natl. Acad. Sci. U.S.A. 95*, 2552−2557.
8. Soubrier, F., Alhenc-Gelas, F., Hubert, C., Allegrini, J., John, M., Tregear, G., and Corvol, P. (1988) Two putative active centers in human angiotensin I-converting enzyme revealed by molecular cloning, *Proc. Natl. Acad. Sci. U.S.A. 85*, 9386-9390.
9. Hubert, C., Houot, A.-M., Corvol, P., and Soubrier, F. (1991) Structure of the angiotensin I-converting enzyme gene. Two

alternate promoters correspond to evolutionary steps of a duplicated gene, *J. Biol. Chem. 266*, 15377−15383.
10. Ehlers, M. R. W., Fox, E. A., Strydom, D. J., and Riordan, J. F. (1989) Molecular cloning of human testicular angiotensin-converting enzyme: the testis isoenzyme is identical to the C-terminal half of endothelial angiotensin-converting enzyme, *Proc. Natl. Acad. Sci. U.S.A. 86*, 7741−7745.
11. Natesh, R., Schwager, S. L., Sturrock, E. D., and Acharya, K. R. (2003) Crystal structure of the human angiotensin-converting enzyme-lisinopril complex, *Nature 421*, 551−554.
12. Hooper, N. M., Keen, J., Pappin, D. J. C., and Turner, A. J. (1987) Pig kidney angiotensin converting enzyme. Purification and characterization of amphipatic and hydrophilic forms of the enzyme establishes C-terminal anchorage to the plasma membrane, *Biochem. J. 247*, 85−93.
13. Wei, L., Alhenc Gelas, F., Soubrier, F., Michaud, A., Corvol, P., and Clauser, E. (1991) Expression and characterization of recombinant human angiotensin I-converting enzyme. Evidence for a C-terminal transmembrane anchor and for a proteolytic processing of the secreted recombinant and plasma enzymes, *J. Biol. Chem. 266*, 5540−5546.
14. Ramchandran, R., Kasturi, S., Douglas, J. G., and Sen, I. (1996) Metalloprotease-mediated cleavage secretion of pulmonary ACE by vasculary endothelial and kidney epithelial cells, *Am. J. Physiol. 271*, H744−H751.
15. Hooper, N. M., Karran, E. H., and Turner, A. J. (1997) Membrane protein secretases, *Biochem. J. 321*, 265−279.
16. Woodman, Z. L., Oppong, S. Y., Cook, S., Hooper, N. M., Schwager, S. L., Brandt, W. F., Ehlers, M. R., and Sturrock, E. D. (2000) Shedding of somatic angiotensin-converting enzyme (ACE) is inefficient compared with testis ACE despite cleavage at identical stalk sites, *Biochem. J. 347*, 711−718.
17. Deddish, P. A., Wang, J., Michel, B., Morris, P. W., Davidson, N. O., Skidgel, R. A., and Erdos, E. G. (1994) Naturally occurring active N-domain of human angiotensin I-converting enzyme, *Proc. Natl. Acad. Sci. U.S.A. 91*, 7807−7811.
18. Deddish, P. A., Wang, L.-X., Jackman, H. L., Michel, B., Wang, J., Skidgel, R. A., Erdös, E. G. (1996) Single-domain angiotensin I converting enzyme (kininase II): characterization and properties, *J. Pharmacol. Exp. Ther. 279*, 1582−1589.
19. Sturrock, E. D., Danilov, S. M., and Riordan, J. F. (1997) Limited proteolysis of human kidney angiotensin-converting enzyme and generation of catalytically active N- and C-terminal domains, *Biochem. Biophys. Res. Commun. 236*, 16−19.
20. Binevski, P. V., Sizova, E. A., Pozdnev, V. F. and Kost, O. A. (2003) Evidence for the negative cooperativity of the two active sites within bovine somatic angiotensin-converting enzyme, *FEBS Lett. 550*, 84−88.
21. Voronov, S., Zueva, N., Orlov, V., Arutyunyan, A., and Kost, O. (2002) Temperature-induced selective death of the C-domain within angiotensin-converting enzyme molecule, *FEBS Lett. 522*, 77−82.
22. Wei, L., Alhenc-Gelas, F., Corvol, P., and Clauser, E. (1991) The two homologous domains of human angiotensin I-converting enzyme are both catalytically active, *J. Biol. Chem. 266*, 9002−9008.
23. Wei, L., Clauser, E., Alhenc-Gelas, F., and Corvol, P. (1992) The two homologous domains of human angiotensin I-converting enzyme interact differently with competitive inhibitors, *J. Biol. Chem. 267*, 13398−13405.
24. Jaspard, E., Wei, L., and Alhenc-Gelas, F. (1993) Differences in properties and enzymatic specificities between the two active sites of human angiotensin I-converting enzyme: studies with bradykinin and other natural peptides, *J. Biol. Chem. 268*, 9496−9503.
25. Danilov, S., Jaspard, E., Churakova, T., Towbin, H., Savoie, F., Lei, W., and Alhenc-Gelas, F. (1994) Structure−function analysis of angiotensin I-converting enzyme using monoclonal antibodies, *J Biol Chem. 269*, 26806−26814.
26. Tzakos, A. G., Galanis, A. S., Spyroulias, G. A., Cordopatis, P., Manessi-Zoupa, E., and Gerothanassis, I. P. (2003) Structure-function discrimination of the N- and C- catalytic domains of human angiotensin-converting enzyme: implications for Cl-activation and peptide hydrolysis, *Protein Eng. 16*, 993−1003.
27. Skirgello, O. E., Binevski, P. V., Pozdnev, V. F., and Kost, O. A. (2005) Kinetic probes for inter-domain cooperation in human somatic angiotensin-converting enzyme, *Biochem. J. 391*, 641−647.
28. Dive, V., Cotton, J., Yiotakis, A., Michaud, A., Vassiliou, S., Jiracek, J., Vazeux, G., Chauvet, M. T., Cuniasse, P., and Corvol, P. (1999) RXP 407, a phosphinic peptide, is a potent inhibitor of angiotensin I converting enzyme able to differentiate between its two active sites, *Proc. Natl. Acad. Sci. U.S.A. 96*, 4330−4335.
29. Cotton, J., Hayaashi, M. A. F., Cuniasse, Ph., Vazeux, G., Ianzer, D., De Camargo, A. C. M., and Dive, V. (2002) Selective inhibition of the C-domain of angiotensin I converting enzyme by bradykinin potentiating peptides, *Biochemistry 41*, 6065−6071.
30. Georgiadis, D., Beau, F., Czarny, B., Cotton, J., Yiotakis, A., and Dive, V. (2003) Roles of the two active sites of somatic angiotensin-converting enzyme in the cleavage of angiotensin I and bradykinin: insights from selective inhibitors, *Circ Res. 93*, 148−154.
31. Sturrock, E. D., Natesh, R., van Rooyen, J. M., and Acharya, K. R. (2004) Structure of angiotensin I-converting enzyme, *Cell. Mol. Life. Sci. 61*, 2677−2686.
32. Tzakos, A. G., and Gerothanassis, I. P. (2005) Domain-Selective Ligand-Binding Modes and Atomic Level Pharmacophore Refinement in Angiotensin I Converting Enzyme (ACE) Inhibitors, *ChemBioChem 6*, 1089−1103.
33. Fernandez, J. H., Hayashi, M. A. F., Camargo, A. C. M., and Neshich, G. (2003) Structural basis of the lisinopril-binding specificity in N- and C-domains of human somatic ACE, *Biochem. Biophys. Res. Commun. 308*, 219−226.
34. Perich, R. B., Jackson, B., Rogerson, F., Mendelson, F. A., Paxton, D., and Johnston, C. I. (1992) Two binding sites on angiotensin-converting enzyme: evidence from radioligand binding studies, *Mol. Pharmacol. 42*, 286−293.
35. Balyasnikova, I. V., Karran, E. H., Albrecht, R. F., II, and Danilov, S. M. (2002) Epitope-specific antibody-induced cleavage of angiotensin-converting enzyme from the cell surface, *Biochem. J. 362*, 585−595.
36. Kost, O. A., Balyasnikova, I. V., Chemodanova, E. E., Nikolskaya, I. I., Albrecht, R. F., II, and Danilov, S. M. (2003) Epitope-dependent blocking of the angiotensin-converting enzyme dimerization by monoclonal antibodies to N-terminal domain of ACE: Possible Link of ACE dimerization and shedding from the cell surface, *Biochemistry 42*, 6965−6976.
37. Balyasnikova, I. V., Woodman, Z. L., Albrecht, R. F., II, Natesh, R., Acharya, K. R., Sturrock, E. D., and Danilov, S. M. (2005) Localization of an N domain region of angiotensin-converting enzyme involved in the regulation of ectodomain shedding using monoclonal antibodies, *J. Proteome Res. 4*, 258−267.
38. Stanislav, M. L., Balabanova, R. M., Alekperov, R. T., Miagkova, M. A., Abramenko, T. V., Kiselev, I. P., Kost, O. A., Nikolskaya, I. I., and Garats, E. V. (2001) Autoantibodies to vasoactive peptides and angiotensin converting enzyme in patients with systemic diseases of the connective tissue, *Ter Arkh.* (Russian) *73*, 20−25.
39. Balyasnikova, I. V., Gavriljuk, V. D., McDonald T. D., Berkowitz, R., Miletich, D. J., and Danilov, S. M. (1999) Antibody-mediated lung endothelium targeting: *In vitro* model using a cell line expressing angiotensin-converting enzyme, *Tumor Targeting 4*, 70−83.
40. Balyasnikova, I. V., Metzger, R., Franke, F. E., and Danilov, S. M. (2003) Monoclonal antibodies to denatured human ACE (CD143): broad species specificity, reactivity on paraffin-section, and detection of subtle conformational changes in the C-terminal domain of ACE, *Tissue Antigens 61*, 49−62.
41. Binevski, P. V., Nikolskaya, I. I., Pozdnev, V. F., and Kost, O. A. (2000) Isolation and characterization of the N-domain of bovine angiotensin-converting enzyme, *Biochemistry (Moscow) 65*, 651−658.
42. Pilliquod, Y., Reinharz, A., and Roth, M. (1970) Studies on the angiotensin-converting enzyme with different substrates, *Biochim. Biophys. Acta 206*, 136−142.
43. Friedland, J., and Silverstein, E. (1976) A sensitive fluorometric assay for serum angiotensin-converting enzyme, *Am. J. Clin. Path. 66*, 416−424.
44. Dixon, M., and Webb, E. C. (1979) *Enzymes*, Longman, London.
45. Cornish-Bowden, A. (1999) pp 306−307, *Fundamentals of Enzyme Kinetics*, Portland Press Ltd, London.
46. Danilov, S. M., Savoie, F., Lenoir, B., Jeunemaitre, X., Azizi, M., Tarnow, L., and Alhenc-Gelas, F. (1996) Development of enzyme-linked immunoassays for human angiotensin I converting enzyme suitable for large-scale studies, *J. Hypertens. 14*, 719−727.
47. Scatchard, G. (1949) The attractions of proteins for small molecules and ions, *Ann. N.Y. Acad. Sci. 51*, 660−672.

48. Towler, P., Staker, B., Prasad, S. G., Menon, S., Tang, J., Parsons, T., Ryan, D., Fisher, M., Williams, D., Dales, N. A., Patane, M. A., and Pantoliano, M. W. (2004) ACE2 X-ray structures reveal a large hinge-bending motion important for inhibitor binding and catalysis, *J. Biol. Chem. 279*, 17996−18007.
49. Thompson, J. D., Higgins, D. G., and Gibson, T. J. (1994) CLUSTAL W: improving the sensitivity of progressive multiple sequence alignment through sequence weighting, positions, specific gap penalties and weight matrix choice, *Nucleic Acids Res. 22*, 4673−4680.
50. Berman, H. M., Westbrook, J., Feng, Z., Gilliland, G., Bhat, T. N, Weissig, H., Shindyalov, I. N., and Bourne, P. E. (2000) The Protein Data Bank, *Nucleic Acids Res. 28*, 235−242.
51. Laskowski, R. A., MacArthur, M. W., Moss, D. S., and Thornton, J. M. (1993) PROCHECK: a program to check the stereochemical quality of protein structures, *J. Appl. Crystallogr. 26*, 283−291.
52. Balyasnikova, I. V., Yeomans, D. C., McDonald, T. B., and Danilov, S. M. (2002) Antibody-mediated lung endothelium targeting: in vivo model on primates, *Gene Ther. 9*, 282−290.
53. Dufour, C., Casane, D., Denton, D., Wickings, J., Corvol, P., and Jeunemaitre, X. (2000) Human-chimpanzee DNA sequence variation in the four major genes of the renin-angiotensin system, *Genomics 69*, 14−26.
54. Mylvaganam, S. E., Paterson, Y., and Gertzoff, E. D. (1998) Structural basis for the binding of an anti-cytochrome antibody to its antigen: crystal structures of Fab E8-cytochrome *c* complex to 1.8Å resolution and FabE8 to 2.26Å resolution, *J. Mol. Biol. 281*, 301−322.
55. Huang, M., Syed, R., Stura, E. A., Sone, M. J., Stefanko, R. S., Ruf, W., Edgington, T. S., and Wilson, I. A. (1998) The mechanism of an inhibitory antibody on TF-initiated blood coagulation revealed by the crystal structures of human tissue factor, Fab 5G9 and TF-5G9 complex, *J. Mol. Biol. 275*, 873−894.
56. Danilov, S. M., Sadovnikova, E., Scharenborg, N., Balyasnikova, I. V., Svinareva, D. A., Semikina, E. L., Parovichnikova, E. N., Savchenko, V. G., and Adema, G. J. (2003) Angiotensin-converting enzyme (CD143) is abundantly expressed by dendritic cells and discriminates human monocyte-derived dendritic cells from acute myeloid leukemia-derived dendritic cells, *Exp. Hematol. 31*, 1301−1309.
57. Muzykantov, V. R., Atochina, E. N., Ischiropoulos, H., Danilov, S. M., and Fisher, A. B. (1996) Immunotargeting of antioxidant enzymes to the pulmonary endothelium, *Proc. Natl. Acad. Sci. U.S.A. 93*, 5213−5218.
58. Atochina, E. N., Balyasnikova, I. V., Danilov, S. M., Granger, D. N., Fisher, A. B., and Muzykantov, V. R. (1998) Catalase targeting to the surface endothelial antigens protects pulmonary vasculature against oxidative insult, *Am. J. Physiol. 275*, L806−L817.
59. Reynolds, P. N., Zinn, K. R., Gavrilyuk, V. D., Balyasnikova, I. V., Rogers, B. E., Buchsbaum, D. J., Wang, M. H., Miletich, D. J., Crizzle, W. E., Douglas, J. T., Danilov, S. M., and Curiel, D. T. (2000) A targetable, injectable adenoviral vector for selective gene delivery to pulmonary endothelium in vivo, *Mol. Ther. 2*, 562−578.
60. Muller, W. H., Brosnan, M. J., Graham, D., Nicol, C. G., Morecroft, I., Channon, K. M., Danilov, S. M., Reynolds, P. N., Baker, A. H., and Dominiczak, A. F. (2005) Targeting endothelial cells with adenovirus expressing nitric oxide synthase prevents elevation of blood pressure in stroke-prone spontaneously hypertensive rats, *Mol. Ther. 12*, 321−327.
61. Danilov, S. M., Martynov, A., Klibanov, A. L., Slinkin, M. A., Sakharov, I. Y., Malov, A. G., Sergienko, V. B., Vedernikov, A. Y., Muzykantov, V. R., and Torchilin, V. P. (1989) Radioimmunoimaging of lung vessels: an approach using 111-In-labeled monoclonal antibody to angiotensin-converting enzyme, *J. Nucl. Med. 30*, 1688−1692.
62. Muzykantov, V. R., and Danilov, S. M. (1995) Targeting of radiolabelled monoclonal antibody against angiotensin-converting enzyme to the pulmonary vasculature, in *Handbook of Targeting Delivery of Imaging Agents* (Torchilin, V. P., Ed.) pp 465−486, CRC, Boca Raton, FL.
63. Danilov, S. M., Faerman, A. I., Printseva, O. Y., Martynov, A. V., Sakharov, I. Y., and Trakht, I. N. (1987) Immunohistochemical study of angiotensin-converting enzyme in human tissues using monoclonal antibodies, *Histochemistry 87*, 487−490.
64. Metzger, R., Bohle, R.-M., Kerkman, L., Eichner, G., Alhenc-Gelas, F., Danilov, S. M., and Franke, F. E. (1999) Distribution of angiotensin I-converting enzyme (CD 143) in the normal human kidney and in non-neoplastic kidney diseases, *Kidney Int. 56*, 1442−1454.
65. Metzger, R., Bohle, R.-M., Chumachenko, P., Danilov, S. M., and Franke, F. E. (2000) CD 143 in the development of atherosclerosis, *Atherosclerosis 150*, 21−31.
66. Franke, F. E., Fink, L., Kerkman, L., Steger, K., Klonisch, T., Metzger, R., Alhenc-Gelas, F., Burkhard, E., Bergmann, M., and Danilov, S. M. (2000) Somatic isoform of angiotensin-converting enzyme in the pathology of testicular germ cell tumors, *Human Pathol. 31*, 1466−1476.
67. Pauls, K., Metzger, R., Steger, K., Klonisch, T., Danilov, S., and Franke, F. E. (2003) Isoforms of angiotensin I-converting enzyme in the development and differentiation of human testis and epididymis, *Andrologia 35*, 32−43.
68. Acharya, K. R., Sturrock, E. D., Riordan, J. F., and Ehlers, M. R. (2004) Ace revisited: a new target for structure-based drug design, *Nat. Rev. Drug Discovery 11*, 891−902.
69. Brown, C. K., Madauss, K., Lian, W., Beck, M. R., Tolbert, W. D., and Rodgers, D. W. Structure of neurolysin reveals a deep channel that limits substrate access, (2001) *Proc. Natl. Acad. Sci. U.S.A. 98*, 3127−3132.
70. Ray, K., Hines, C. S., Coll-Rodriguez, J., and Rodgers, D. W. (2004) Crystal structure of human thimet oligopeptidase provides insight into substrate recognition, regulation, and localization, *J. Biol. Chem. 279*, 20480−20489.
71. Comellas-Bigler, M., Lang, R., Bode, W., and Maskos, K. (2005) Crystal structure of the E. coli dipeptidyl carboxypeptidase Dcp: further indication of a ligand-dependent hinge movement mechanism, *J. Mol. Biol. 349*, 99−112.
72. Arndt, J. W., Hao, B., Ramakrishnan, V., Cheng, T., Chan, S. I., and Chan, M. K. (2002) Crystal structure of a novel carboxypeptidase from the hyperthermophilic archaeon Pyrococcus furiosus, *Structure (Cambridge) 10*, 215−224.
73. Kim, H. M., Shin, D. R., Yoo, O. J., Lee, H., and Lee, J. (2003) Crystal structure of Drosophila angiotensin I-converting enzyme bound to captopril and lisinopril, *FEBS Lett. 538*, 65−70.
74. Fernandez, J. H., Neshich, G., and Camargo, A. C. M. (2004) Using bradykinin-potentiating peptide structures to develop new antihypertensive drugs, *Genet. Mol. Res. 3*, 554−563.

BI052591H